



Faculty of Bioscience Engineering
Academic year 2010 – 2012

Influence of membrane fouling on the removal of pharmaceutical

Bui Thao Nguyen

Promotor: Prof. dr. ir. Arne Verliefde

Tutor: Oranso Themba Mahlangu

Master's dissertation submitted in partial fulfillment of the requirements for
the degree of
Master in Environmental Sanitation

COPYRIGHT

'The author and the promoter authorize consultation and partial reproduction of this thesis for personal use. Any other reproduction or use is subject to copyright protection. Citation should clearly mention the reference of this work.'

'De auteur en de promoter geven toelating deze thesis voor consultative beschikbaar te stellen en delen ervan te kopiëren voor persoonlijk gebruik. Elke ander gebruik valt onder de beperkingen van het auteursrecht, in het bijzonder met betrekking tot de verplichting de bron te vermelden bij het aanhalen van resultaten uit deze scriptie.'

Gent, August 2012

The promoter

De promoter

Prof. Dr. ir. Arne Verliefde

The author

De auteur

Bui Thao Nguyen

ACKNOWLEDGEMENTS

First and foremost, I would like to express my sincere gratitude to my promoter **Prof. dr. ir. Arne Verliefde** for giving me an opportunity to work in the Laboratory of the Department of Applied Analytical and Physical Chemistry. His good advices and support have been invaluable on my academic achievement.

I would especially thank to my tutors, **Oranso Themba Mahlangu** and **Arnout Dhaese** for their unreserved support and guidance during the whole thesis research.

I am deeply grateful to **Prof. dr. ir. Paul Van der Meeren** who gave background about membrane through the course Membrane Technology in Environmental Treatment.

Thank **Quenten Denon** for repairing the pilot set-up and the TOC analyser. Especially, all staffs in the lab have always created such a wonderful working environment and for that, I thank all of them.

I am also grateful to the **Prof. M. Van der Heede** and **Coordinators** of Centre for environmental Sanitation for assisting me in many different ways throughout the two years of the master programme.

Last but not the least, I wish to thank **my parents, little brother** and **two cousin** who have always supported, encouraged and believed in me. I dedicate this thesis to them.

Bui Thao Nguyen

August 2012

ABBREVIATIONS

Abbreviation	Description
NF	Nanofiltration
MF	Microfiltration
UF	Ultrafiltration
RO	Reverse Osmosis
CECP	Cake enhanced concentration polarization
CP	Concentration polarization
TMP	The applied pressure
$\Delta\pi$	The osmosis pressure
MWCO	Molecular weight cut off
SA	Sodium alginate
SD	Standard deviation
WWTP	Wastewater treatment plant
DLS	Dynamic light scattering
PCS	Photon correlation spectroscopy
TOC	Total organic carbon

TABLE OF CONTENTS

CHAPTER 1: INTRODUCTION	1
CHAPTER 2: LITERATURE REVIEW	3
2.1. MEMBRANE TECHNOLOGY	3
2.1.1. The growth of membrane technology	3
2.1.2. Principles of membrane separation and classification	4
2.2. MEMBRANE FOULING	6
2.2.1. The problems of membrane operation.....	6
2.2.2. Concentration polarization and fouling.....	7
2.3. MEMBRANE FOULING MECHANISMS	11
2.3.1. Increased hydraulic resistance.....	12
2.3.2. Cake-enhanced concentration polarisation.....	12
2.4. ORGANIC SOLUTE REJECTION BY MEMBRANES	14
2.4.1 Conventional treatment over RO/NF membranes.....	14
2.4.2 Organic solute rejection by NF/RO membranes	15
2.4.3 Qualitative rejection prediction of organic solutes	16
2.5. THEORETICAL BACKGROUND AND MEMBRANE TRANSPORT MODELS – QUANTITATIVE REJECTION PREDICTION.....	18
2.5.1. Membrane transport models.....	18
2.5.2. Determination of hindrance factors K_c and K_d	21
2.5.3. Determination of the solute partition coefficient ϕ	21
2.6. GOAL OF THIS THESIS	22
CHAPTER 3: MATERIALS AND METHODS	24
3.1. MEMBRANE FILTRATION SET UP AND EXPERIMENTAL PROTOCOL	24
3.1.1. Cross-flow filtration set-up and experimental protocol.....	24
3.1.2. Dead-end filtration set-up and filtration protocol.....	26

3.2.	CHEMICALS AND REAGENTS	27
3.2.1.	Model foulants	27
3.2.2.	Model pharmaceutical	29
3.2.3.	Other chemicals.....	31
3.3.	NANOFILTRATION MEMBRANE.....	32
3.3.1.	Membrane properties	32
CHAPTER 4: RESULTS AND DISCUSSION		24
4.1.	INFLUENCE OF MEMBRANE FOULING ON PERMEATE FLUX.....	35
4.1.1.	Permeate flux of clean membrane	35
4.1.2.	Fouling by aluminum oxide	36
4.1.3.	Fouling by latex.....	37
4.1.4.	Fouling by sodium alginate	39
4.1.5.	Fouling by combined foulants.....	41
4.2.	EFFECTS OF MEMBRANE FOULING ON INORGANIC SALT REJECTION.....	42
4.2.1.	Salt rejection of clean membrane	42
4.2.2.	Salt rejection of fouled membranes.....	43
4.3.	REJECTION OF CARBAMAZEPINE	46
4.3.1	Rejection of carbamazepine by clean membrane	46
4.3.2	Rejection of carbamazepine by fouled membranes.....	47
4.4.	CARBAMAZEPINE-MEMBRANE AFFINITY	50
CHAPTER 5: CONCLUSIONS AND RECOMMENDATIONS.....		24
5.1.	CONCLUSIONS	53
5.2.	RECOMMENDATIONS FOR FUTURE WORKS	54

LIST OF TABLES

Table 2.1: Overview of liquid pressure driven membrane processes	5
Table 3.1: Concentrations of foulants for experimental runs	28
Table 3.2: Properties of Carbamazepine	30
Table 3.3: Some properties of membrane given by manufacturer	32
Table 4.4: Surface tension components and the free-energy of interactions for clean and fouled membranes	50

LIST OF FIGURES

Figure 2.1: Schematic representation of a two-phase system separated by a membrane	4
Figure 2.2: Flux behavior as a function of time	6
Figure 2.3: Concentration polarization profile under steady-state conditions	8
Figure 2.4: Flux as a function of time for both concentration polarization and fouling	10
Figure 2.5: Overview of various types of resistances towards mass transport across a membrane in pressure driven process	11
Figure 2.6: Flow chart for prediction of rejection of organics by high pressure membranes	18
Figure 3.1: Nanofiltration set-up for rejection experiments with selected membranes	25
Figure 3.2: Filtration protocol for fouling/rejection experiments	26
Figure 4.1: Relative flux as a function of time for clean membrane	35
Figure 4.2: Relative flux as a function of time for fouling experiment with $Al_2O_3 + CaCl_2$	36
Figure 4.3: Relative flux as a function of time for latex fouling experiments with and without $CaCl_2$	38
Figure 4.4: Relative flux as a function of time for SA fouling experiment with and without $CaCl_2$	40
Figure 4.5: The evolutions of permeate fluxes in combined fouling experiments	41
Figure 4.6: Salt rejection for clean membrane as a function of time	43
Figure 4.7: The reduction of salt rejection of clean membrane and different fouled membrane	44
Figure 4.8: Experimental values for carbamazepine rejection by the clean membrane as a function of time	47

Figure 4.9a: Carbamazepine rejection behavior of fouled membrane with the absence of CaCl ₂	47
Figure 4.9b: Carbamazepine rejection behavior of fouled membrane with the presence of CaCl ₂	48
Figure 4.9c: Carbamazepine rejection behavior of fouled membrane with combined foulants	48
Figure 4.10: Comparison between the reduction of salt rejection and carbamazepine rejection.....	49
Figure 4.11: The reductions of salt rejection and carbamazepine rejection vs. interaction energy.....	52

ABSTRACT

The occurrence of pharmaceuticals in water bodies has become an increasing concern, particularly due to possible problems related to human health effects. However, these pollutants are not completely removed by conventional water treatment plants and even state-of-the-art high pressure membrane filtration installations sometimes demonstrate incomplete removal. Therefore, the aim of this study was to elucidate mechanisms affecting pharmaceutical removal by high pressure membranes, and to evaluate the impact of membrane fouling on this removal. The widely used pharmaceutical carbamazepine was used as a model solute, and an NF 270 membrane was chosen as representative membrane. Aluminum oxide, sodium alginate, latex and their combinations were used as model foulants to simulate fouling in nanofiltration process. These foulants were chosen to mimic foulants naturally present in surface water. Filtration and fouling experiments were conducted in the presence and absence of divalent cations, since these are known to aggravate membrane fouling. The membranes and foulants were further characterized to elucidate the effects of (physico-chemical properties of) the fouling layers on rejection of carbamazepine and salts. It was observed that membrane fouling by latex resulted in a very severe flux decline, but the effects on salt rejection and carbamazepine rejection were minor. Sodium alginate fouling, on the other hand, resulted in less flux decline, but did cause significant reductions in both salt and carbamazepine rejections. Cake-enhanced concentration polarization was found to play a crucial role in the rejection of salts and carbamazepine. Surprisingly, free energies of interaction between carbamazepine and the fouled membranes did not correlate very well with the determined rejection. This is most likely caused by the overwhelming effect of cake-enhanced concentration polarization.

CHAPTER 1

INTRODUCTION

Recently, there has been an increasing concern about the emergence of trace organic contaminants in the water resources worldwide. These pollutants include pharmaceutically active compounds, endocrine disrupting compounds and personal care products. They are present in municipal sewage, mainly as a result of improper human disposal. In some cases, pesticides are also detected in drinking water resources due to agricultural run-offs [1]. However, there is limited knowledge regarding health problems associated with consumption of water contaminated with trace amounts of these pollutants.

During the last decades, high pressure membrane processes such as nanofiltration (NF) and reverse osmosis (RO) became widely employed mainly in new water treatment systems. Currently, NF/RO membranes are mostly employed for the production of high quality potable water which conventional treatment plants not using membranes cannot produce. Although NF/RO are very promising for the removal of organics, traces of some of the pollutants are still detected in the effluent of NF/RO membrane systems. Moreover, it has been observed in many NF and RO plants that this incomplete rejection efficiency can even be aggravated membrane fouling, which is an inevitable phenomenon in full-scales applications. Many studies on membrane fouling have been carried out [2-13] because the accumulation of foulants on the membrane surface result in serious operational problems, such as a decline in permeate flux and a resulting energy increase. However, less studies have clearly focused on the underlying mechanisms of the effects of fouling on rejection of trace organic compounds. The latter is a difficult research field, mainly due to the complexity of the mixtures and the variability in the characteristics of organic compounds to be rejected, the foulants and the membranes. Therefore, there is a need to further investigate the effect of membrane fouling by different foulants (separately, but more interestingly when they co-exist in the

same solution with others) on rejection of organic compounds. This is very important as it generally represents the situation in real NF/RO applications.

Therefore, this dissertation was aimed at investigating the influence of membrane fouling on the removal of the model pharmaceutical carbamazepine in surface water applications. Three types of foulants were used to foul the membrane. One type of organic foulants was used (sodium alginate, mimicking biopolymers in surface water), and two types of inorganic foulants, mimicking colloids in surface water. Fouling experiments were performed with each foulant existing solely in the feed water and also in the presence of other foulants. The observed permeate flux and salt rejection as a function of time were used to determine the magnitude of fouling. The membrane and foulants characteristics were carefully determined, to see if a correlation could be found between the physico-chemical characteristics of the foulants and the pharmaceuticals, and the observed flux declines and changing rejection values.

CHAPTER 2

LITERATURE REVIEW

2.1. MEMBRANE TECHNOLOGY

2.1.1. The growth of membrane technology

There has been a significant growth in development and application of membrane technology in the last few decades. Currently membrane processes such as microfiltration, nanofiltration, ultrafiltration and reverse osmosis are used in a wide range of applications, in sectors such as food and beverages, metallurgy, pulp and paper, textile, pharmaceutical, dairy, biotechnology and in the chemical industry [14]. This increase in use is mainly due to the rise in environmental concerns about water quality and scarcity, since membrane technology has been recognized as one of the applications that could be used to provide safe water from impaired sources such as seawater desalination, surface water treatment and reclamation of wastewater. This makes potable water and wastewater treatment plants the largest markets for membrane consumption, accounting for nearly half of the sales. Demand for membranes globally has reached €13 billion yearly and 2012, and an average percent annual rise is further expected. The BRIC countries (Brazil, Russia, India and China) and other countries which are arranged as strongly developing industries and/or under stress of water resources will see the fastest growth of membrane technology. In terms of regional distribution, North America will occupy the largest membrane market. However, the growth will be limited in many developing countries, particularly in Africa and parts of South Asia, due to the still hefty capital investment costs that are required. The largest investments in membrane technology for water treatment (mainly seawater desalination) are currently found in the Middle East, to guarantee sufficient water supply for drinking, agriculture and industries [15].

2.1.2. Principles of membrane separation and classification

There are several types of membrane processes dependent on the driving force that is used. In all processes, the membrane acts as a (semi-permeable) barrier between two phases, and the membrane controls the passage of different chemical substances from one phase to the other. The separation process is dependent on the characteristics of both the chemical substances that need to be retained and the membrane.

A preferential passage of solvent molecules through the membrane, versus a dedicated limited passage of solute molecules, leads to a reduction in concentration of that solute in the produced water (the permeate) and an increase in the feed water if filtration is carried in a full recirculation mode. Figure 2.1 shows a schematic representation of a typical membrane separation process.

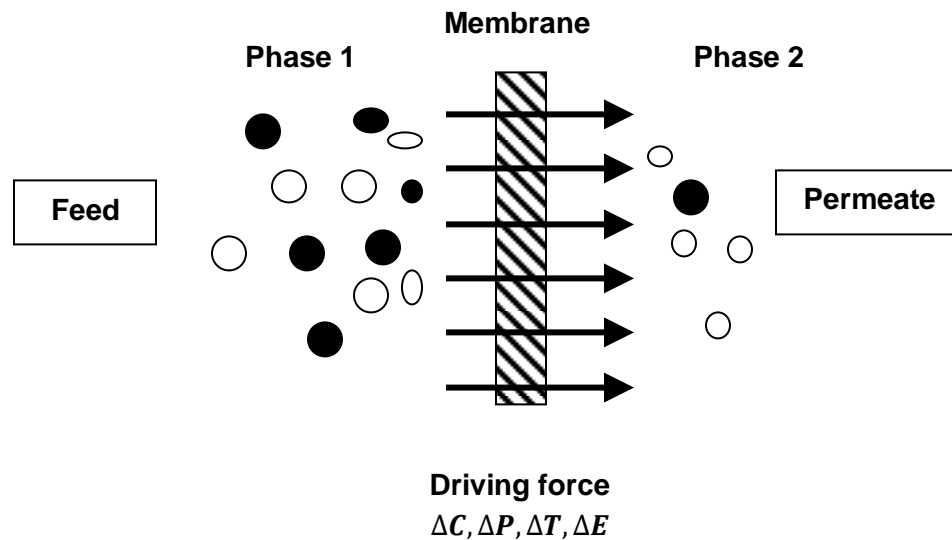


Figure 2.1: Schematic representation of a two-phase system separated by a membrane

As can be seen in Figure 2.1, by application of a driving force to the components in the feed side, transportation through the membrane takes place. The driving force can be a chemical potential difference or an electrical potential difference as a result of differences in either applied pressure, solute concentration, temperature,

and/or electrical potential between the different sides of the membrane. Pressure-driven membrane processes are the most common in water treatment.

Pressure-driven membrane systems are classified based on several factors, including the materials from which they are made, their physical configurations and pore sizes, and the conditions under which the systems are operated. The most used criteria in pressure-driven membrane processes are the pore size and or the applied transmembrane pressure. As such, pressure-driven membrane processes are grouped into microfiltration (MF), ultrafiltration (UF), nanofiltration (NF) and reverse osmosis (RO) membranes [14,16]. Table 2.1 presents an overview of these pressure driven membrane processes.

Table 2.1: Overview of liquid pressure driven membrane processes

Name	Pore size	Pressure (bar)	Permeability (l/h/m ² /bar)	Mechanism	Separation of
MF	0.05 – 10 μ m	0.1 – 2	> 50	Sieving	Particles
UF	1 – 50 nm	1 – 5	10 – 50	Sieving	Macromolecules (10-100kDa)
NF	About 1 nm	5 – 20	1 – 15	Sieving Exclusion	Organic compounds (200 – 1000 kDa); salts
RO	Nonporous	10 – 100	0.05 – 1.5	Dissolution Diffusion	Organic compounds; salts

Microfiltration (MF) and ultrafiltration (UF) are the most commonly used membrane processes in water treatment. Their application is in the removal of contaminants such as particles and macromolecules. Basically, the pollutants include suspended solids, turbidity, some colloids, bacteria, protozoa and viruses. MF and UF membrane systems also serve as pretreatment for nanofiltration and reverse osmosis.

Nanofiltration (NF) and reverse osmosis (RO) are employed for the rejection of low molecular weight solutes such as inorganic salts and dissolved organics, due to their

small pore sizes. Due to their higher membrane resistance, a much higher pressure must be applied to force the same amount of solvent through the membrane. NF and RO are often considered as one process because they have the same basic principles of separation (see further).

Although NF/RO membranes may serve as good candidates for the removal of organics, unfortunately their operation can be greatly affected by membrane fouling which has been reported to cause membranes performing poorly [2,48].

2.2. MEMBRANE FOULING

2.2.1. The problems of membrane operation

Membrane performance in terms of flux and solute removal (rejection) can change significantly with time. A typical flux behaviour as a function of time is shown in Figure 2.2.

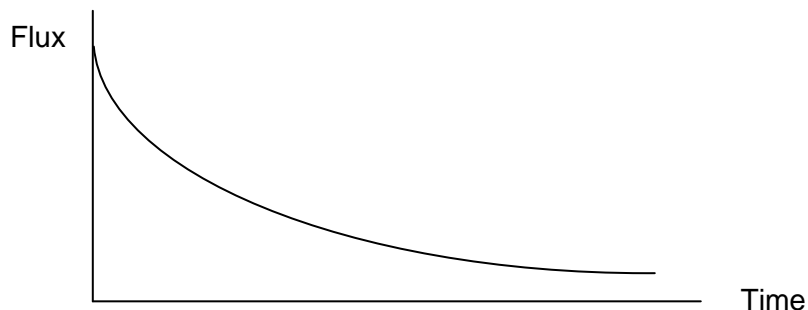


Figure2.2: Flux behavior as a function of time

Flux decline during separation is one of the most crucial reasons why membrane filtration processes are not more extensively used, since it results in increased pumping costs, higher costs for membrane cleaning and thus has a negative influence on the economics of a membrane [14].

Concentration polarization and membrane fouling are the main causes of membrane flux decline. The former occurs directly and is reversible when flux is alleviated while the later is long-term and irreversible. These two phenomena result from the nature of both

membrane and the feed, and by interactions between the membrane and the feed. These phenomena are also dependent on other factors such as solute concentration, particle size, pH and ionic strength of the feed, as well as the fluid shear forces [17].

2.2.2. Concentration polarization and fouling

2.2.2.1. Concentration polarization

In pressure-driven membrane applications, water is transported through the membrane by an applied hydraulic pressure. However, as water is transported towards the membrane, also the dissolved solutes are transported towards the membrane surface. The solvent permeates through the membrane while the solutes are (partially) rejected by the membrane. As a result, the rejected solute can accumulate at the membrane surface, leading to a higher concentration of the solute at the membrane surface. Due to this concentration build-up, there will be a driving force for diffusion of the solute away from the membrane surface, back to the bulk of the feed (so-called back diffusion). This back-diffusion is accelerated by a higher cross-flow velocity or a greater turbulence at the membrane surface, since this increases mass transfer. After a short time of operation, a steady-state condition will be established whereby the convective solute flow to the membrane surface exactly equals the diffusive solute flow away from the membrane surface to the bulk (in some cases plus the solute flux through the membrane if the membrane is not completely selective). In this steady-state mechanism, there will still be a slightly higher concentration of solutes at the membrane surface compared to the bulk. This phenomenon is called concentration polarization [14,17]. The concentration profile that has been established is schematically shown in Figure 2.3.

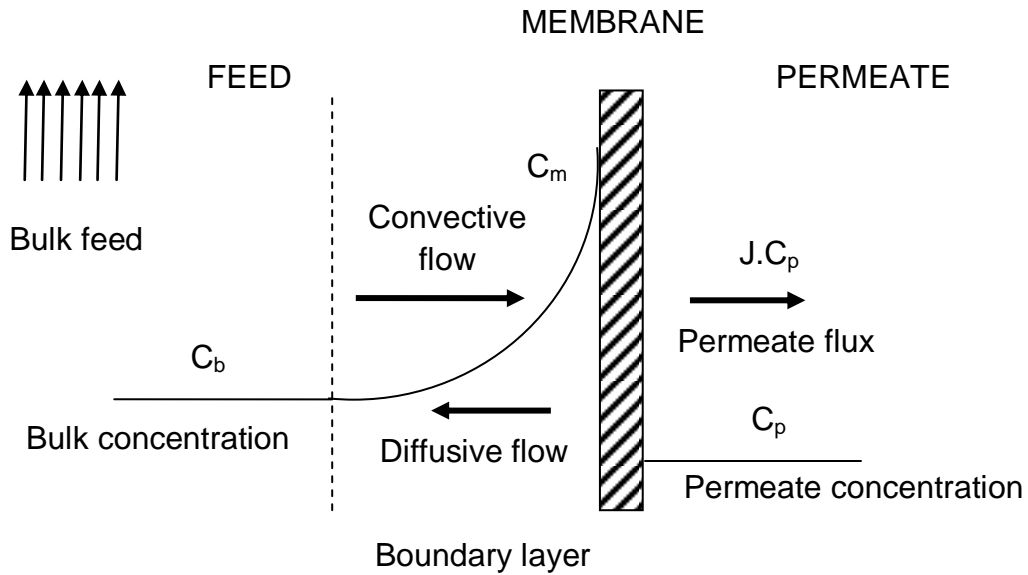


Figure 2.3: Concentration polarization profile under steady-state conditions

The accumulation of solute within the concentration polarization (CP) layer can be presented by the convection-diffusion equation:

$$J * C = J * C_p - D * \frac{dC}{dy} \quad (2.1)$$

where

- J : the solvent flux
- C : the solute concentration in the bulk
- C_p : the solute concentration in the permeate
- D : the diffusion coefficient

For spherical particles, the diffusion coefficient follows the Stokes-Einstein equation:

$$D_o = \frac{k_B T}{3\pi\mu d_p} \quad (2.2)$$

where

- K_B : the Boltzmann constant
- T : the absolute temperature

Due to concentration polarization, the osmotic pressure difference that exists between the feed and the permeate side of the membrane, due to solute rejection, is aggravated since the concentration at the membrane surface increases.

The concentration polarisation modulus β is equal to the ratio of the solute concentration at the membrane surface (c_m) compared to the bulk fluid (c_b). It is given by the following equation:

$$\beta = \frac{c_m}{c_b} = \exp\left(\frac{J}{k}\right) = \exp\left(\frac{J \cdot \delta}{D}\right) \quad (2.3)$$

Normal flux in a pressure-driven membrane process is given by:

$$J = \frac{\Delta P - \Delta\pi}{\mu * R_m} \quad (2.4)$$

where $\Delta\pi$ is the osmotic pressure, R_m is the membrane resistance.

When concentration polarisation is present, the osmotic pressure difference between feed and permeate becomes higher, due to the increased concentration in the feed. As a result, the actual flux becomes smaller:

$$J = \frac{\Delta P - \beta\Delta\pi}{\mu * R_m} \quad (2.5)$$

2.2.2.2. Membrane fouling

Basically, if no membrane fouling occurs, the flux remains constant as a function of time when steady state conditions for concentration polarization have been reached. However, a continuous downward-trend in flux is often observed, which can be explained by membrane fouling phenomena (see Figure 2.4). Membrane fouling can be defined as the irreversible deposition of retained particles, colloids, emulsions, suspensions, macromolecules, salts and other foulants on or in the membrane, and can only be removed by chemical cleaning. In UF and MF, fouling can sometimes be removed by backwashing, but this is not possible in NF and RO applications.

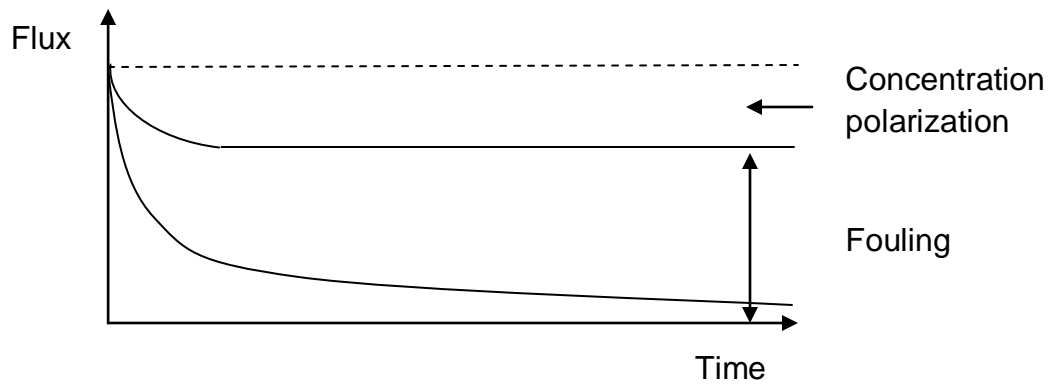


Figure 2.4: Flux as a function of time for both concentration polarization and fouling

When the flux decline disappears by using pure water instead of the feed solution, the flux decline is reversible and should not be considered as fouling, but is mainly the result of concentration polarization [18]. Membrane fouling itself is not reversible when just flushing with clean water. Membrane fouling includes adsorption, pore blocking, gel layer formation and concentration polarization, which is described in the Figure 2.5.

In fact, fouling is basically an increase in membrane resistance due to the accumulation on the membrane surface. Thus, the total resistance is constituted of all the above resistances. In the ideal case where no fouling occurs, the only resistance is the membrane resistance R_m . Through the filtration, however, the accumulation of solutes near the membrane surface causes a highly concentrated layer near the membrane and this layer forms a concentration polarization resistance. When the solute concentration becomes too high, a gel layer can be formed and this refers to a gel layer resistance R_g . Moreover, the solute particles can penetrate to the membrane pores and block these pores which lead to a formation of pore-blocking resistance R_p . Finally, adsorption can happen at the membrane surface and within the pore, R_a , and thus causes a rise in the total resistance [14].

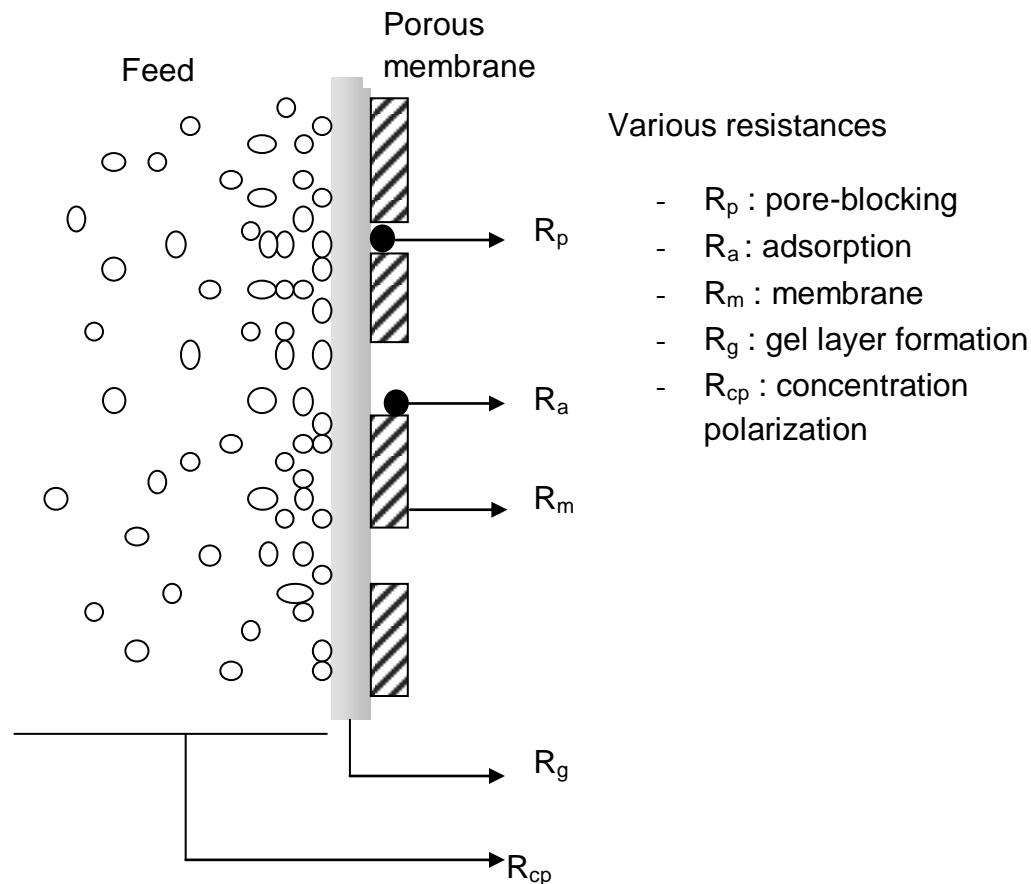


Figure 2.5: Overview of various types of resistances towards mass transport across a membrane in pressure driven process.

2.3. MEMBRANE FOULING MECHANISMS

As mentioned above, fouling is a major problem influencing the operational performance of the membrane, membrane stability and also energy cost. Despite many efforts to reduce membrane fouling, for example, by improvement of membrane properties, optimization of hydraulic conditions, and pretreatment of influent water, fouling is often still inevitable. The phenomenon of fouling is very complex and difficult to describe. Fouling depends on physical and chemical parameters, involving foulant concentration, temperature, pH, ionic strength and specific interactions [14].

Fouling is mainly an accumulation of solids or dissolved solids on the membrane surface. This can lead to an increased hydraulic resistance, which limits the driving force

that can actually be applied to drive water through the membrane. In addition, for NF and RO membranes, flux decline can also be caused by another mechanism, the so-called “cake-enhanced concentration polarization”.

2.3.1. Increased hydraulic resistance

The membrane resistance model can be employed to describe the permeate flow through a membrane (see Equation 2.4). If the fouling layer only consists of equal-sized spherical particles, the specific cake resistance (i.e. the resistance per unit cake thickness) is usually predicted using the Carman-Kozeny equation:

$$\widehat{R}_c = \frac{180\mu(1 - \varepsilon_c)}{\rho_p d_p^2 \varepsilon_c^3} \quad (2.6)$$

where

- ε_c : the cake layer porosity
- ρ_p : the solid density of the particle
- d_p : the particle diameter

From this equation, it is predicted that a reduction in cake porosity and particle diameter lead to a rise of the specific cake layer resistance. Of course, also as the thickness of the cake increases, the membrane resistance will increase.

In practice, however, cake resistances are not that easy to calculate, since most cakes do not only exist out of ideal spherical-shaped particles. Therefore, it is difficult to predict the extra hydraulic resistance R_c due to fouling.

2.3.2. Cake-enhanced concentration polarisation

Since NF and RO are salt rejection membranes, there will always be an increase of salts at the membrane surface (concentration polarization). This concentration polarization is

usually kept under control by a cross-flow alongside the membrane, which creates back-diffusion of salts to the bulk.

However, when NF and RO membranes get fouled by colloids and/or organic foulants, the presence of these foulants can actually increase the concentration polarization of the salts, since the back-diffusion of the salts is limited by the foulant cake on the membrane surface. This increased concentration polarization results in an increase in osmotic pressure difference across the membrane, and thus a decreased driving force for water transport.

Mathematically, the increase in concentration polarization due to fouling, can be represented by a change in the diffusion coefficient of the salts in the concentration polarization model shown above. When there is a presence of a cake layer on the membrane surface, the back-diffusion of smaller solutes (such as salts, which have a high osmotic pressure) is hindered by the presence of the cake layer due to the tortuous pathway of transport. This results in a hindered diffusion coefficient D^* for back diffusion. This hindered diffusion coefficient is related to the original diffusion coefficient, but also to the porosity and the tortuosity of the cake layer and can be written as follows:

$$D^* = \frac{D_o \varepsilon}{\tau^2} \quad (2.7)$$

The slower back diffusion due to the smaller diffusion coefficient (smaller porosity and higher tortuosity lead to smaller diffusion) results in a faster accumulation of salts solutes and therefore creates a higher concentration in the cake layer. This cake-enhanced concentration polarization (CECP) is not only an important contributor to membrane flux decline (mainly observed in colloidal fouling of NF and RO membranes), but is often also accompanied by a drop of salt rejection over time (as a result of the concentration of salt at the membrane surface going up).

Cake-enhanced concentration polarization, however, is not only limited to salts: with dissolved organic compounds which are small enough and able to penetrate the (colloidal) cake layer, CECP may also happen. As a consequence, the concentration of

organic solutes such as pharmaceuticals in the cake layer can also increase, leading to lower rejection values (see below) [3].

2.4. ORGANIC SOLUTE REJECTION BY MEMBRANES

Since membranes are often used for production of water from impaired water sources, and impaired water sources are often polluted by trace organic chemicals such as pesticides, pharmaceuticals, etc., it is important that these organic solutes are well removed by the membranes

2.4.1 Conventional treatment over RO/NF membranes

Pharmaceuticals are developed to enhanced human health, but recently they have become one of the notorious water pollutants [1,19]. A wide range of drug brands such as antibiotics, anti-depressants, tranquillizers, cancer treatment pills and pain killers have been detected in different water bodies at high concentrations [20]. Main sources of these pollutants are hospitals, pharmaceutical industries and medical facilities as well as households which dispose solutions of these contaminants directly into the drain without treatment. Due to their polarity, persistence and water solubility, they are able to pass through waste water treatment plants (WWTP). Their low adsorption on sludge and soil may cause contamination of surface and ground waters. Although it is argued that pharmaceuticals are not a problem to human beings due to their very low concentrations, it is believed that long-term exposure to pharmaceuticals and similar compounds is likely to interfere with hormone production. Moreover, the life of aquatic flora and fauna are at great risk. As an evidence of this, anti-depressants have been blamed for altering sperm levels and spawning patterns in marine life. Therefore, many studies of pharmaceuticals in water mainly focus on aquatic animals [21].

In conventional wastewater treatment plants, the removal of antibiotics fluctuates greatly. Nevertheless, several organic compounds are removed by some activated sludge treatment processes via hydrolysis, biotransformation or sorption onto flocs, suspended solid or activated sludge and then separated by sedimentation [22,23]. The

removal efficiency of pharmaceutical pollutants is also influenced by the operating conditions of the treatment process, such as temperature, hydraulic retention time (HTR) and particularly solid retention time (STR). Due to high health risks associated with ingestion of pharmaceuticals, there is a need to remove them in source water before it is consumed by some of the removal processes (both advanced and tertiary) including tertiary media filtration, ozonation, chlorination, UV radiation, activated carbon adsorption and NF/RO filtration. Sand filtration and UV disinfection are less efficient in removing almost all antibiotics. However, NF and RO membrane filtration processes are much more effective in rejecting pharmaceuticals under optimal operation.

2.4.2 Organic solute rejection by NF/RO membranes

Organic solute rejection by membranes is dependent on a number of things, such as hydrodynamic effects, concentration, pH and background electrolyte. However, the most important factor is the solute-membrane interactions at the membrane interface. Indeed, solute-membrane interactions are the key factors to determine the rejection of organic solutes by membrane. These interactions include steric hindrance, solute-membrane non-electrostatic affinity (often mistakenly referred to as hydrophobic interactions) and electrostatic interactions. These solute-membrane interactions are mainly dependent on solute and membrane physico-chemical properties, although process conditions and feed water composition may play a role as well [4,24].

The first solute-membrane interaction is steric hindrance which is primarily a sieving mechanism, and is thus mainly determined by membrane pore size and solute size: solutes with a size larger than the membrane pore size are efficiently rejected, whereas solutes with a smaller size can easily pass through the membrane. This mechanism results in a typical sigmoidal (S-shaped) curve when rejection is plotted as a function of the solute size or solute molar mass. This S-shape (instead of a step-curve) results from the fact that the membrane has a certain pore size distribution around the average pore size [25].

Solute-membrane non-electrostatic affinity interactions typically include hydrophobic attraction, hydrogen bonding and dielectric effects which are mainly determined by solute and membrane physicochemical parameters. These interactions might have an influence on the rejection, in addition to the steric hindrance. Solutes with high affinity to membrane will be able to partition into the membrane matrix and diffuse through the membrane, and finally leads to a lower rejection values. From a study conducted by Verliefde et al [26], they demonstrated that there is a dramatic influence of solute-membrane affinity on organic rejection by NF and RO membranes.

The third factor that also plays a crucial role in the rejection of organic solutes is electrostatic interactions. Electrostatic interactions occur between charged solutes and charged functional groups of the membranes. On the membrane surface, functional groups may be carboxyl groups, amine groups and many others. In practice, most NF and RO membranes are negatively charged due to the overwhelming presence of carboxylic acid functional groups.

2.4.3 Qualitative rejection prediction of organic solutes

In order to predict the rejection of a solute by NF or RO membranes, it is essential to know the contributions of the different physico-chemical interaction mechanisms. Therefore, a number of physical/chemical properties of solute and membrane as well as solution chemistry have to be carefully considered. These physic-chemical properties include molecular size, charge, hydrophobicity of the solute, pore size, membrane morphology, membrane and solute charge and membrane hydrophobicity.

Bellona et al. (2004) developed a simple flow chat (see Figure 2.6) that can be qualitatively used to predict rejection of organics by high pressure membranes [28]. By using the flow chart, one can initially estimate the rejection efficiency of NF/RO for non-charged and negatively charged organic solutes. The organic compounds are classified based on different physico-chemical characteristics including charge (based on the acid constant)), hydrophobicity (expressed as the logarithm of the octanol-water partitioning coefficient) and molecular size, in order to identify the main mechanisms responsible for

rejection. Based on this diagram (which is based on a wide experimental database), the dominant mechanisms of rejection can be determined and the rejection qualitatively estimated when the physico-chemical characteristics of the solute and membrane are known. The diagram is followed from the top to the bottom and incorporates the effect of different physico-chemical characteristics of solute and membrane and also operating conditions, for example the pH of feed water (since this determines the charge properties). The general rejection prediction is given in qualitative terms of high, moderate or low rejection; determined after passing through several levels of parameter decisions.

Although this diagram is the useful tool for qualitative prediction of organic compounds by membrane filtration, there are some limitations in its applicability for predicting chemical behavior in real – full scale treatment system. Firstly, it is mainly used for a qualitative estimation, while a quantitative estimation which is an extremely important aspect of rejection is not involved. A further limitation of the membrane diagram is that it only accounts for increased rejections due to electrostatic repulsion between the negatively charged solutes and negatively charged membranes. In a study performed on negatively charged membranes by Verliefde et al. [26], it was concluded that electrostatic attractive forces may also occur between positively charged solutes and the negatively charged membrane surface. These attractions result in the accumulation of the positively charged solutes at the membrane surface and create an extra concentration-polarization effect, leading to lower rejections of the positively charged solutes.. Another drawback is that $\log K_{ow}$, as a descriptor of solute hydrophobicity, is used to determine affinity interactions of the solute with the membrane. This is a serious flaw, since $\log K_{ow}$ only takes hydrophobic interactions into account. A final drawback of the qualitative model, is that it does not take effects of membrane fouling into account.

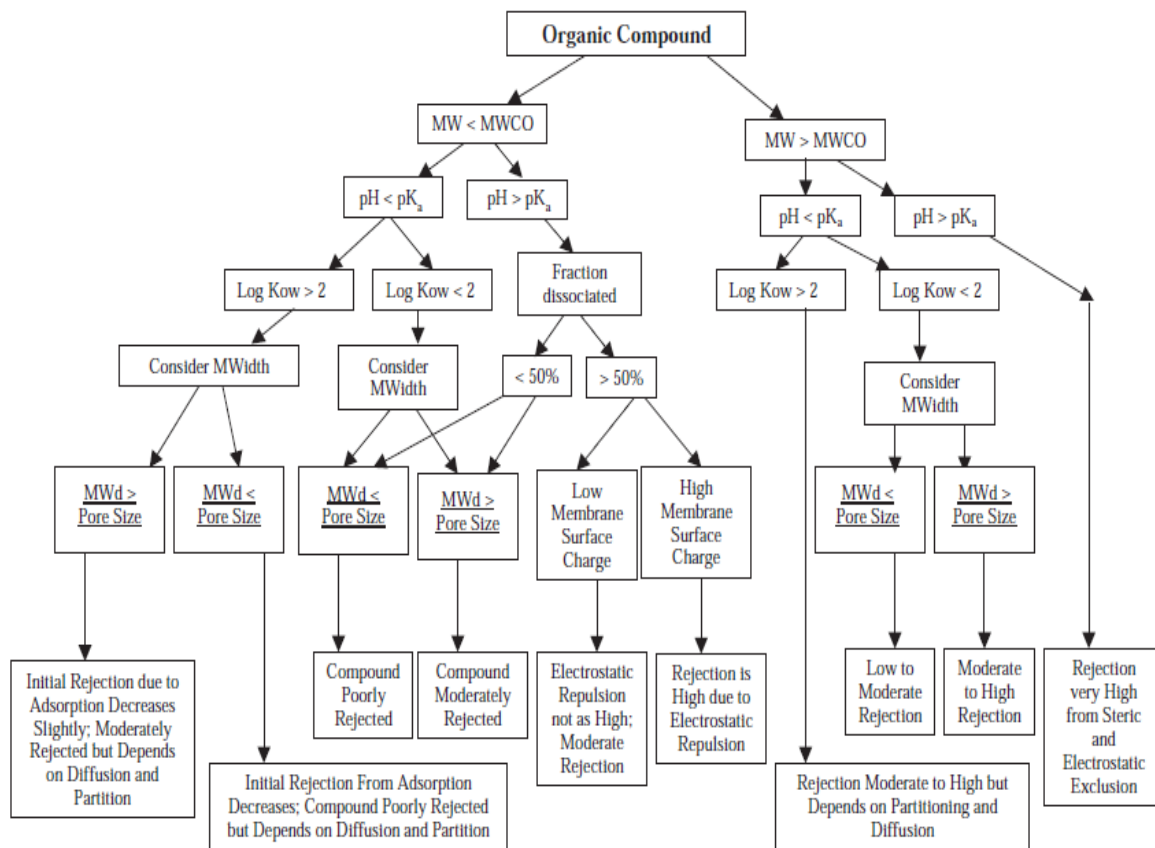


Figure 2.6: Flow chart for prediction of rejection of organics by high pressure membranes

2.5. THEORETICAL BACKGROUND AND MEMBRANE TRANSPORT MODELS – QUANTITATIVE REJECTION PREDICTION

2.5.1. Membrane transport models

To cope with the limitations of the qualitative rejection graph of Bellona et al., more quantitative rejection models were developed over time. In the recent years, consensus has been reached on the fact that transport through NF/RO membranes can be best described by convection-diffusion models for pore transport. The most comprehensive transport model for solutes through high-pressure membranes is the extended Nernst-Planck equation, which gives the basic description of the transport of ions and organic

solutes through the membranes (in fact the membrane pores). The equation is written as (2.8):

$$J_s = -D_p \frac{dc}{dx} - \frac{zcD_p}{RT} F \frac{dv}{dx} + \frac{J_v}{\varepsilon} K_c c \quad (2.8)$$

Where

- J_s and J_v : respectively the solute and solvent flux,
- ε : the membrane porosity
- $D_p = K_d D_\infty$: the solute diffusion coefficient in the membrane
- D_∞ : the solute diffusion coefficient in water
- c : the solute concentration
- x : the axial position within the membrane
- K_c : the hindrance factor against convection transport
- K_d : the hindrance factor against diffusive transport
- z : valence of ion
- R : gas constant
- T : absolute temperature ($^{\circ}\text{K}$)
- F : Faraday constant (Cmol^{-1})

The terms on the right hand side represent solute transport due to diffusion, the electric field gradient and convection respectively.

For uncharged (organic) solutes, the effects of the electric field gradient can be neglected. In these cases, the solute flux equation simplifies to the well-known Spiegler-Kedem model, which states that transport of uncharged solute through nanofiltration and reverse osmosis membranes can be presented by irreversible thermodynamics by a combination of diffusive and convective transport [16,29] :

$$J_s = \langle V \rangle C_p = -D_p \frac{dc}{dx} + \frac{J_v}{\varepsilon} K_c \quad (2.9)$$

where $\langle V \rangle$ is the average fluid velocity in pores ($\langle V \rangle = \frac{J_v}{\varepsilon}$) and C_p is the solute bulk permeate concentration.

In order to obtain an expression for solute rejection, Equation 2.9 needs to be integrated with the following boundary conditions, which use the solute partition coefficient ϕ . The solute partition coefficient is the ratio of the solute concentration inside the membrane pore over the solute concentration in the feed, so it describes whether a solute will easily penetrate into the membrane or not. As such, it is probably the most important parameter determining solute rejection.

Thus,

- $x = 0$ (within the membrane at feed side):

$$C_{x=0} = C_f = \phi C_m = \phi \beta C_f \quad (2.10)$$

- $x = \Delta x$ (within the membrane at lower surface):

$$C_{x=\Delta x} = C_p = \phi C_p \quad (2.11)$$

where

- Δx : the membrane thickness
- β : the hydrodynamic concentration polarization
- c_f : the solute concentration in the membrane matrix at the feed side
- c_p : the solute concentration in the membrane matrix at the permeate side
- C_f : the solute feed concentration in the bulk
- C_p : the solute permeate concentration in the bulk
- C_m : the solute feed concentration at the membrane surface

After integration, equation 2.9 becomes:

$$R = 1 - \frac{C_p}{C_f} = 1 - \frac{\beta \phi K_c}{1 - ((1 - \phi K_c) \exp(-Pe))} \quad (2.12)$$

where the Peclet number, Pe is defined as:

$$Pe = \frac{J_v K_d \Delta x}{K_d \varepsilon D_\infty} \quad (2.13)$$

Equation (2.12) can be used to predict solute rejection by clean NF and RO membranes, given that the values of all constants in the equation are known.

2.5.2. Determination of hindrance factors K_c and K_d

In this study, the membrane is assumed to be porous with uniformed pores. If the solute velocity profile is fully developed inside the membrane pores with a parabolic Hagen-Poiseuille profile, these hindrance factors for convection and diffusion can be calculated as [16]:

$$K_c = (2 - (1 - \lambda)^2) (1 + 0.054\lambda - 0.988\lambda^2 + 0.441\lambda^3) \quad (2.14)$$

$$K_d = 1 - 2.3\lambda + 1.154\lambda^2 + 0.224\lambda^3 \quad (2.15)$$

Where $\lambda = r_s/r_p$ which is the ratio of solute to pore radius.

2.5.3. Determination of the solute partition coefficient ϕ

The solute partitioning coefficient is given by the following equation:

$$\phi = (1 - \lambda)^2 \exp\left(-\frac{\Delta G_i}{kT}\right) \quad (2.16)$$

Where k is the Boltzmann constant, T is the absolute temperature (in °K) and ΔG_i is the free-energy difference associated with the differences in interactions of the solute in the water phase and the membrane phase. The partition coefficient therefore depends on ΔG_i and the steric hindrance (expressed by the factor $(1-\lambda)^2$). ΔG_i can be used as a quantification of attractive or repulsive solute-membrane affinity interactions. If ΔG_i is negative, transport of the solute to the membrane will be facilitated since the solute has a high affinity for the membrane; when ΔG_i is positive, the solute will be repelled by the membrane and partitioning will be less. Only when $\Delta G_i = 0$, the traditional models which only consider the size exclusion effects apply. It is clear that ΔG_i thus has a large influence on rejection. When there is less partitioning, rejection is higher.

ΔG_i can be calculated based on the surface tensions of the solute (S), membrane (M) and liquid (L):

$$\begin{aligned} \Delta G_i &= A\Delta G_{SLM} \\ &= 2 \left[\begin{aligned} &\sqrt{\gamma_S^{LW}\gamma_L^{LW}} + \sqrt{\gamma_M^{LW}\gamma_L^{LW}} - \sqrt{\gamma_S^{LW}\gamma_M^{LW}} - \gamma_L^{LW} \\ &+ \sqrt{\gamma_L^+}(\sqrt{\gamma_S^-} + \sqrt{\gamma_M^-} + \sqrt{\gamma_L^-}) - \sqrt{\gamma_S^+\gamma_M^-} + \sqrt{\gamma_L^-}(\sqrt{\gamma_S^+} + \sqrt{\gamma_M^+} - \sqrt{\gamma_L^+}) - \sqrt{\gamma_S^-\gamma_M^+} \end{aligned} \right] \end{aligned} \quad (2.17)$$

In which γ_i^{LW} is the apolar (Lifshitz-van der Waals) component of the surface tension, γ_i^+ and γ_i^- are the electron – acceptor and electron – donor component of surface tension, respectively. If water is used as a solvent, the values for γ_L^{LW} , γ_L^+ and γ_L^- are known from literature. The remaining surface tension components for the membrane and the solute can be calculated by contact angle measurements via the Dupré Young equation:

$$(1 + \cos\theta)\gamma_L = 2 \left(\sqrt{\gamma_M^{LW}\gamma_L^{LW}} + \sqrt{\gamma_M^+\gamma_L^-} + \sqrt{\gamma_M^-\gamma_L^+} \right) \quad (2.18)$$

Where θ is the contact angle measured between a droplet of liquid L on the membrane surface. By repetition of contact angle measurements with 3 different liquids with known surface tension components and then solving the set of 3 equations, the surface tension components of the membrane and compressed plates of solutes can be determined.

2.6. GOAL OF THIS THESIS

The objective of this thesis research is investigate the influence of fouling on the removal of carbamazepine by the nanofiltration membrane process. Carbamazepine is chosen as model pharmaceutical because it is one of pharmaceuticals that have the highest concentration appearing in European surface waters [30]. Three model foulants (aluminum oxide, latex and sodium alginate) are used. Aluminum oxide and latex are model substitutes for inorganic colloids found in surface and waste water, whereas sodium alginate acts as a model for biopolymers found in these water types. Aluminum oxide and latex have different charge properties (the former positively charge, the latter negative), to elucidate if charge effects play a role in membrane fouling and the

influence on rejection. The membranes are fouled by these substituents separately, and also by mixtures of these foulants. Fouling is monitored by the temporal changes of flux and salt rejection. By spiking carbamazepine during the fouling runs, the influence of fouling on carbamazepine rejection is also determined.

To investigate if the surface energy approach developed to model rejection for clean membranes (see Equations (2.17) to (2.18)) is also valid for fouled membranes, the interaction energies between carbamazepine and the fouled membranes will be determined and related to rejection behavior.

This study is mainly conducted on a small laboratory scale set-up with flat sheet membrane coupons in a cross-flow mode. In addition, dead-end experiments are also carried out to obtain smooth fouling layers for easier characterization of the membrane surface properties.

MATERIALS AND METHODS

3.1. MEMBRANE FILTRATION SET UP AND EXPERIMENTAL PROTOCOL

3.1.1. Cross-flow filtration set-up and experimental protocol

3.1.1.1. *Set-up*

A laboratory-scale cross-flow reverse osmosis set-up was used in this study (Figure 3.1). The pilot RO installation (Boerenbond, Agro-Industries, Leuven, Belgium) consists of a cylindrical membrane cell in which the membranes are packed in circular plate-and-frame modules, in a sandwich like structure. The total effective surface area of the membrane is 0.04 m². For each fouling experiment, a new membrane piece was used to eliminate the influence of the previous experiments.

The feed solution is delivered to the cell from a reservoir (10L) by a piston pump. The concentrate flow rate was monitored by a rotameter. The feed pressure and cross-flow velocity were controlled by means of a bypass valve and back pressure regulator. The feed water temperature was kept constant (25 ± 2 °C) using a temperature controller equipped with a stainless steel heater exchanger coil, which was submerged directly to the feed reservoir. The concentrate and permeate fluxes were recycled back to the feed. The permeate, was collected in a volumetric flask and timed to measure permeate flux.

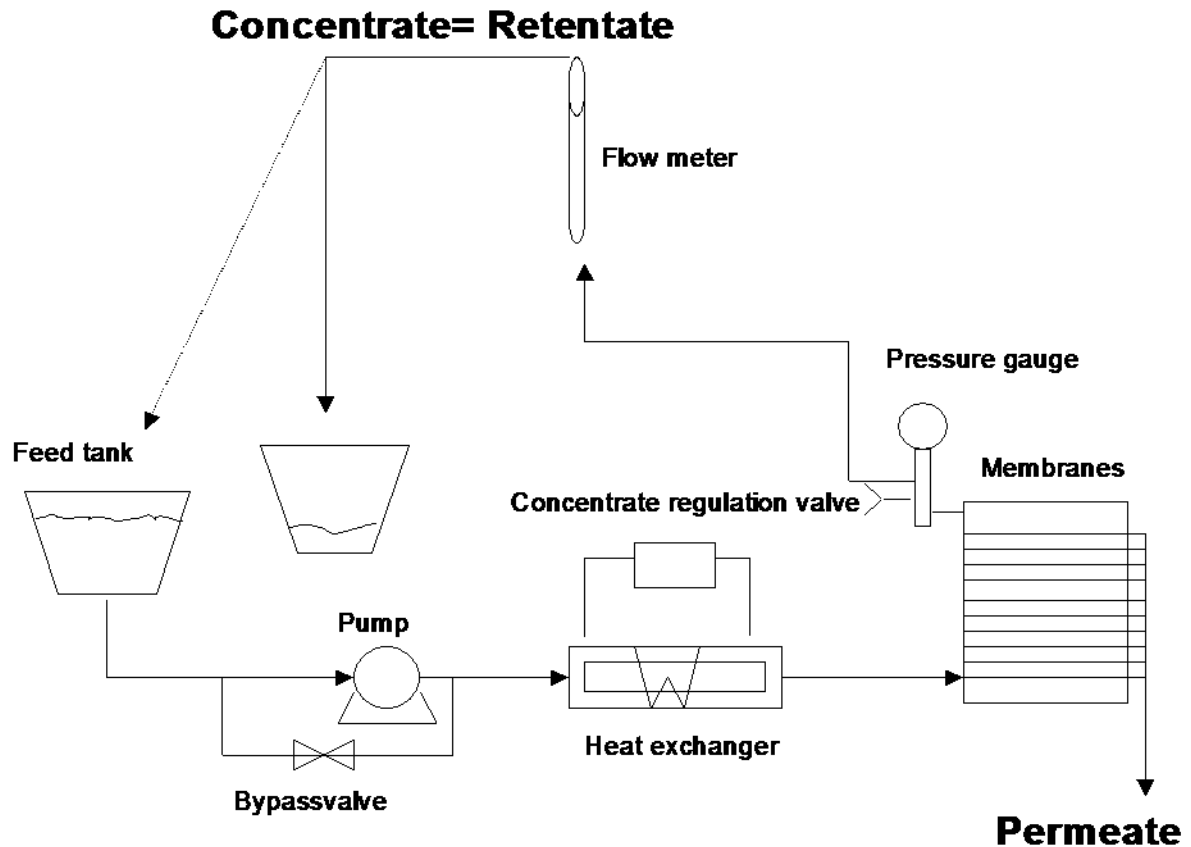


Figure 3.1: Nanofiltration set-up for rejection experiments with selected membranes

3.1.1.2. Filtration protocol

Membrane fouling and subsequent retention experiments were conducted in two steps: a first compaction step, followed by the actual and fouling run and rejection measurement. A schematic of the filtration protocol depicts in Figure 3.2. Firstly, the membrane was compacted using Milli-Q water at 8 bars in 2 hours or until the flux stabilized. The In the next stage, a mixed solution containing electrolyte (10 mM NaCl), carbamazepine (10 mg/l) and foulants were introduced to the feed reservoir and the cross-flow velocity was adjusted to 0.2 m/s and the pressure was fixed at 3bars (300kPa).

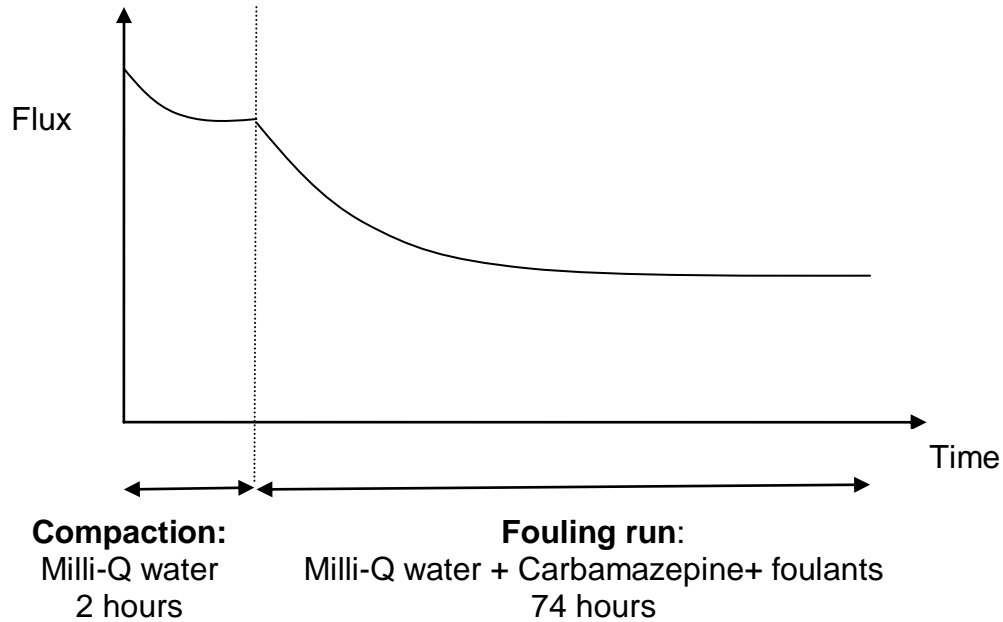


Figure 3.2: Filtration protocol for fouling/rejection experiments

In these experiments, the fouling layer on the membrane surface was developed during the filtration experiments which mean that the foulants and pharmaceutical were dosed homogeneously at the start. This is the situation which is the most representative for practical membrane operation. Foulants were at first added separately to access single foulant effect. They were then dosed in different combinations to evaluate the effect of combined fouling on the permeate flux, the rejection of salt and the pharmaceutical (carbamazepine). The experiment was run for 74h and the pH of the feed solution (approximately 7.0) was adjusted.

The permeate samples were collected in glass vials with stoppers and stored in the 4°C refrigerator before analysis of carbamazepine as total organic carbon.

3.1.2. Dead-end filtration set-up and filtration protocol

Due to the specific structure of the plastic frames used for the cross-flow mode, and due to the washing off by the cross-flow velocity, fouled membranes from the cross-flow unit

had a non-uniform distribution of the cake layer. Therefore, it was difficult to characterize this cake by characteristic analyses, including contact angle and streaming potential measurements. To solve this problem, dead-end experiments were carried out on lab-scale, to achieve denser and more uniform fouling layers. A membrane of a required diameter of 51mm was cut and placed at the bottom of the unit. After sealing the unit, it was pressured up to 10 bar using N₂.

The filtration was run for 4 hour period, which allowed a thick layer of foulants accumulated on the membrane. The fouled membranes were then removed from this filtration system and then put on a desiccator in 24 hours. Contact angle measurements were performed to determine surface properties of the fouled membranes and then calculate the free energy of interactions between the solute and membranes.

3.2. CHEMICALS AND REAGENTS

3.2.1. Model foulants

Latex, Sodium Alginate and Aluminum oxide were used as model foulants in the following experiments.

Latex is a liquid which extracted by some plants or trees, particularly rubber trees. It is being used in many different applications such as adhesives, inks, paints, coating, drug delivery systems, floor polish, films, carpet packing and so on [31]. Colloidal Latex was obtained from EOC group, Industrial park, B9700 Oudenaarde. It was supplied at 50% suspension in water and was successively stored in a refrigerator at 4°C.

Sodium alginate was supplied by Sigma – Aldrich (Product of United Kingdom).It was originally extracted from brown algae. Sodium alginate (SA) was employed as a model constituent of polysaccharide, one of the most ubiquitous constituents of extracellular polymeric substances (EPS) in the secondary wastewater effluent. Its molecular weight reported by the manufacturer is 10 – 60 kDa or 8291 g/mol.

Commercial aluminum oxide Al_2O_3 colloids were employed as model colloids in the fouling experiments. It was provided as 30% suspension by Evonik Degussa GmbH (Hanau-Wolfgang, Belgium) with pH value of 3.0 – 5.0 and the density of 1.26 g/m^3 .

In order to investigate the effects of the selected foulants in the presence of divalent ions, calcium chloride (CaCl_2) was added to the feed solution. Table 3.1 summarizes foulants chemistry used for the fouling experiments in this study.

Table 3.1: Concentrations of foulants for experimental runs

Fouling experiments	Concentration (mg/l)			
	Al_2O_3	SA	Latex	CaCl_2
Al_2O_3	30	-	-	-
$\text{Al}_2\text{O}_3 + \text{CaCl}_2$	30	-	-	2
SA	-	20	-	-
SA + CaCl_2	-	20	-	2
Latex	-	-	30	-
Latex + CaCl_2	-	-	30	2
$\text{Al}_2\text{O}_3 + \text{SA} + \text{CaCl}_2$	30	20	-	2
Latex + SA + CaCl_2	-	20	30	2

3.2.1.1. Zeta potential measurements of the foulants

The value of the zeta potential describes the potential stability of the colloidal system. If particles in suspension have a large negative or positive zeta potential, they will tend to repel each other and no flocculation occurs. These particles are said to be stable. The dividing line between stable and unstable suspension is generally put at either +30mV or -30mV [11].

The zeta-potential of the individual colloids and the alginate molecules as function of pH were measured by a Zetasizer2C (Malvern Instruments, United Kingdom). The particles and molecules were suspended in electrolyte (10 mM of KCl), prepared with deionized water. The electrolyte's pH was adjusted with either hydrochloric acid or sodium hydroxide.

The Zetasizer determines the electrophoretic mobility of particles in a solution. The electrophoretic mobility refers to a velocity of a particle in an electric field. Zeta potential was calculated from measured electrophoretic mobility by using the Helmholtz-Smoluchowski Equation 3.1:

$$U_E = \frac{2\varepsilon z f(ka)}{3\eta} \quad (3.1)$$

Where z is zeta potential, U_E is electrophoretic mobility, ε and η are dielectric constant and viscosity respectively, and $f(ka)$ is the Henry's function.

3.2.1.2. Particle size measurements of the foulants

Particles were measured by the photon correlation spectroscopy (PCS 100M, Zetasizer 2C, Malvern Instruments, England). The measurement is based on laser light scattering. Particles in a light beam will scatter light into space, with angles and intensities which depend on the particle size, the optical properties of these particles, the light source and their suspending medium. The Zetasizer 2C has a resolution between 0.05 μm and 3.5 mm.

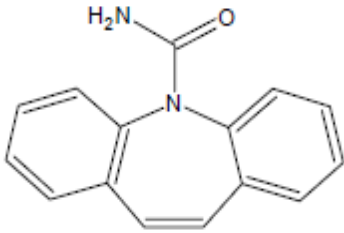
3.2.2. Model pharmaceutical

Carbamazepine was chosen in this study as a model pharmaceutical. $\text{C}_{15}\text{H}_{12}\text{N}_2\text{O}$ is the formula of carbamazepine and its molecular weight is 236.28 g/mol [10,32]. Carbamazepine is a widely used anti-epileptic drug and considered as a representative pharmaceutically active compound. It is often found at trace levels in many different water resources [34]. In practice, this pharmaceutical can be quite persistent to the conventional biological sewage treatment process [22]. However it be removed effectively by nanofiltration or reverse osmosis filtration. Moreover, carbamazepine is

also representative of the emerging trace organic contaminants commonly encountered in secondary treatment effluent and sewage treatment [35].

A stock solution of carbamazepine (1 g/l) was prepared in Milli-Q water, stored at 4°C and used within 1 month. In this study, carbamazepine was used at a concentration of 10 mg/l for all experiments. The purity of this chemical was reported to be 90% or higher. Some typical properties of carbamazepine are given in the Table 3.2.

Table 3.2: Properties of Carbamazepine

Properties of Carbamazepine	Carbamazepine
Solubility, mg/l	121
pK _a	13.9
Log K _{ow}	2.45
Charge at pH 7	Neutral
Molecular weight, g/mol	236.28
Molecular width ¹ , nm	0.507
Molecular height ¹ , nm	0.529
Molecular length ¹ , nm	0.891
Molecular structure	

¹ Reference source: [10]

In order to evaluate the rejection of the non-ionizable pharmaceutical carbamazepine by clean and fouled membranes, the TOC concentration of carbamazepine in permeate samples were measured during the experimental runs. Since the degradation or volatilization of carbamazepine did not occur in the relatively long period of experiments (74 hours), the feed concentration was assumed to be constant throughout the experiments. TOC measurements were conducted in 24 hours after samples were collected.

Carbamazepine concentration was measured as TOC using a Total organic carbon (TOC) analyzer (Shimadzu TOC-VCSH, Shimadzu Scientific Instruments, USA). The TOC analyser was calibrated for TC and IC using concentrations of 100 ppm TC and 20 ppm IC. Feed and permeate samples were analysed for TOC and rejection was calculated using Equation 3.2.

$$R_i = 1 - \left(\frac{c_{p,i}}{c_{f,i}} \right) \quad (3.2)$$

Where i is the solute of interest, and R_i , $c_{p,i}$, and $c_{f,i}$ are the rejection, the permeate and feed concentrations of solute i respectively. All samples were analyzed immediately after the collection of the last sample.

To make sure that carbamazepine was the only compound responsible for TOC in the permeate, blank experiments without addition of carbamazepine were carried out, which showed negligible TOC in the permeate. This indicates that the rejection of sodium alginate and other foulants is 100%, which was also expected based on their size compared to the membrane pore size.

3.2.3. Other chemicals

Sodium chloride (supplied by VWR International bvba/sprl) was used to prepare the background electrolytes for the feed solutions. Calcium chloride (supplied by Merck Eurolab nv/sa) was employed to investigate the influence on the fouling rate of selected foulants. These chemicals were dosed at 10 mM and 2 mg/l respectively.

Salt concentrations (sodium chloride) in the feed and permeate were measured using a conductivity meter (Consort K612, Belgium). Salt rejection was also calculated by Equation 3.1 with $c_{p,i}$ and $c_{f,i}$ being conductivity of permeate and feed respectively. In the concentration region used (10 mM of NaCl), salt concentration is linearly to conductivity. Therefore, conductivity of the feed and permeate water were measured to calculate salt rejection following previous research works [36].

All solutions and feed water were prepared with Milli-Q water which had conductivity of less than 1 μ S/cm at room temperature.

3.3. NANOFILTRATION MEMBRANE

3.3.1. Membrane properties

A low salt-rejection thin-film composite nanofiltration membrane (NF 270) was selected for this study. The NF 270 membrane was supplied by Dow-FilmTec, Minneapolis. The membrane is a typical nanofiltration membrane with wide applications in the drinking water production [37]. The membrane has a polyamide skin layer on top of a polysulphone/polyester support layer. Some properties of the membrane as given by the manufacturer are presented in Table 3.3:

Table 3.3: Some properties of membrane given by manufacturer

Properties of NF 270 membrane	Value
PWP ¹ at 25°C, L/m ² .h.bar	12
MWCO, Da	200 – 300
Rejection (%)	
-MgSO ₄	>97
-NaCl	~50
-CaCl ₂	40 - 60
Max operating pressure, bar	41
Max operating temperature, °C	45
Pore size ² , nm	0.71 ± 0.14
PWP ¹ is the pure water permeability	
Pore size ² : reference [38].	

As soon as it was received, the membrane was immediately stored in a refrigerator prior to use at 4 °C. Prior to fouling experiments, sufficient membrane samples were cut from

the flat sheet roll and soaked in deionized (DI) water at room temperature for at least 48h to remove preservation liquids present in the membrane.

3.3.2. Membrane characterization

3.3.2.1. Streaming potential measurements

The electrokinetic properties of a membrane describe the electrical characteristics of membrane surface. These properties were measured by means of streaming potential measurements [39]. By studying the streaming potential of the membrane at a certain range of pH, the membrane surface isoelectric point can also be identified. Streaming potential is the electrical potential discrepancy when there is a relative motion between a fluid containing charged species and charged surface due to hydrostatic pressure gradient [40].

Measurements were performed on clean membrane as a function of pH in the range of 3.0 to 10.0. The background electrolyte was 10mM potassium chloride (KCl) and the pH was adjusted with small quantities of 1 M sodium hydroxide (NaOH) and 1M hydrochloric acid (HCl).

The zeta potential and the streaming potential are related by the Helholtz-Smoluchowski equation (3.3)

$$\zeta = \frac{\eta K \Delta E}{D \epsilon_0 \Delta P} \quad (3.3)$$

Where ζ is the apparent zeta potential, D is the dielectric constant of the medium, ϵ_0 is the permittivity of vacuum, η and K are the viscosity and conductivity of the bulk solution, respectively, and $\Delta E/\Delta P$ is the streaming potential developed as a result of an applied pressure gradient [41].

3.3.2.2. Contact angle measurements

Contact angle measurements were used to determine surface tension properties of the membranes. Contact angle measurements with probe liquids were carried out using the sessile drop method. The three probe liquids with well-known surface tension properties that were used are ultrapure water, diiodomethane and glycerol. These liquids are chosen on the premise that two must be polar (ultrapure water and glycerol) and one must be apolar (diiodomethane) [42].

Sessile drop measurements were carried out using a commercial contact angle analyser and drop shape analysis software (Kruss, Germany. Model: DSA 10-MK2). In order to minimize the influence of surface morphology on the contact angle, at least 10 measurements were carried out for each liquid on each membrane sample and the average of the measurements was taken. Membrane samples were dried in a desiccator for 24 h prior to contact angle analysis. The measured contact angles were then used for the calculation of surface tension components and free energy of solute-membrane interaction, according to [42].

Surface tension components of carbamazepine were determined in a similar manner, by carrying out contact angle measurements on a compressed plate of pharmaceutical powder.

3.3.2.3. Scanning electron microscopy (SEM)

In order to identify the morphology of the membrane surface, the scanning electron microscopy (SEM) technique was used. For the purpose of this study, images of the top surface (active layer) and the bottom (support layer) of the membrane were taken. Membrane species were first dried in a desiccator for 24 h before the coupons were sent to the Department of Materials Science and Engineering (Technologiepark, Zwijnaarde, Belgium) for analysis. Membrane samples were sputter-coated with gold before analysis.

RESULTS AND DISCUSSION

4.1. INFLUENCE OF MEMBRANE FOULING ON PERMEATE FLUX

4.1.1. Permeate flux of clean membrane

Permeate flux results with the NF270 membranes are described in this section. Results are reported in terms of relative flux as a function of time. The relative flux (J_R) is the flux at any time (J_i) during the fouling test divided by the initial flux (J_o): $J_R(\%) = (1 - J_i/J_o) * 100\%$.

The evolution of flux for the filtration of pure water with background electrolyte (so the clean membrane baseline, see Figure 4.1) shows a relatively stable flux, although it does slightly decline over time (relative flux dropped from 100% to 97.9%). The very slight reduction of permeate flux in the experiment with the clean NF 270 membrane can most probably be explained by membrane compaction, although an increased concentration of the background electrolyte might play a role as well: some permeate samples are taken over time to measure conductivity and flux. This leads to a slight reduction in volume of the feed water, and since permeate samples contain less salt (due to salt rejection by the membrane), the concentration of the salts in the feed water increases. This might indeed lead to a lower flux, because of a higher osmotic pressure. However, this effect is only expected to be minor and the main reason for the slight flux decline in the absence of foulants is expected to be membrane compaction due to the high applied pressure.. This type of flux decline for a virgin membrane has also been mentioned in previous publications [4,9,36,44]. It will also be seen in the fouling experiments.

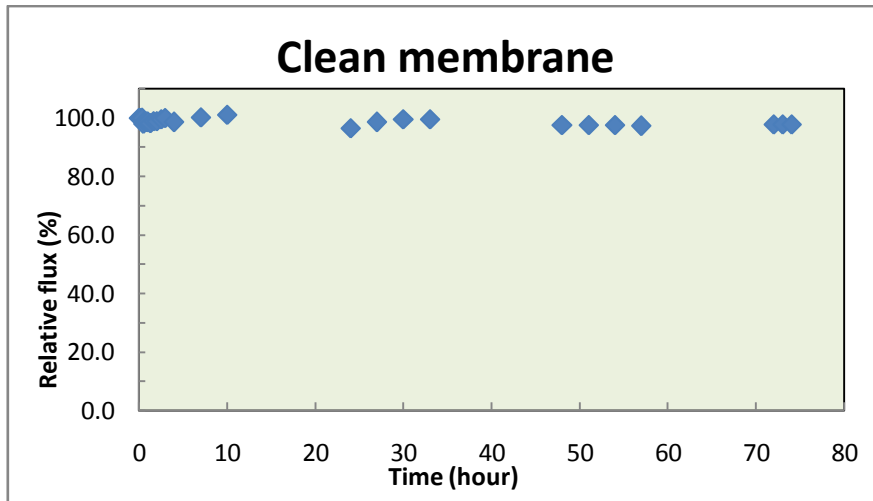


Figure 4.1: Relative flux as a function of time for clean membrane

4.1.2. Fouling by aluminum oxide

Experimental data for the membranes fouled by aluminum oxide with and without the addition of calcium chloride in the electrolyte are presented in Figure 4.2. In general, the presence of alumina colloids in the feed did not result in a significant flux decline compared to the clean membrane. Also the addition of CaCl_2 did not significantly affect this permeate flux.

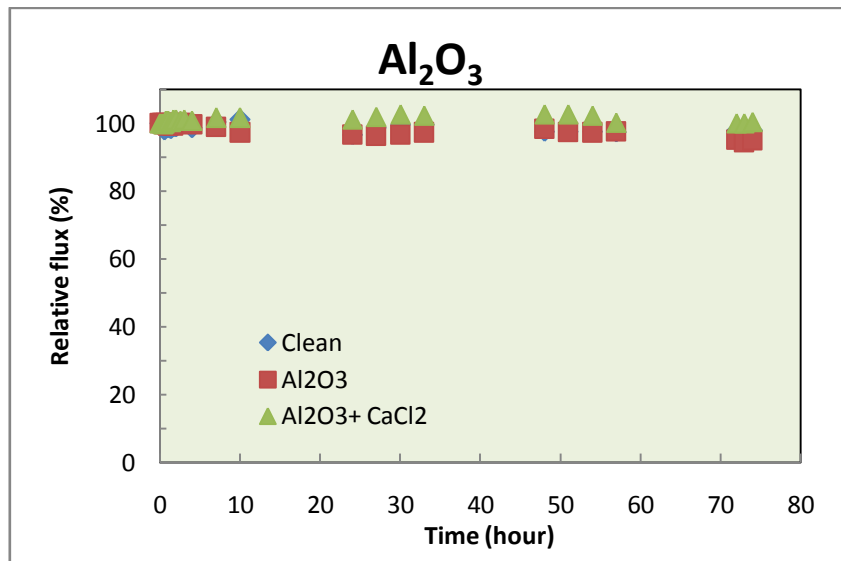


Figure 4.2: Relative flux as a function of time for fouling experiment with $\text{Al}_2\text{O}_3 + \text{CaCl}_2$

There are several possible explanations that could be used to explain the flux data of the aluminum oxide fouling experiment. The first explanation would be that there is hardly any deposition of Al_2O_3 colloids on the membrane surface. From visual observations with the bare eye, no clear fouling layer could be distinguished on the membrane. It is however not very plausible that positively charged Al_2O_3 particles (see appendix for Al_2O_3 characterisation) would not interact with the negatively charged membrane (see appendix for membrane surface charge characterization). It is possible that a stable monolayer coverage of the membrane by Al_2O_3 was formed due to charge attraction between the membrane and the Al_2O_3 particles, but that further development of the Al_2O_3 cake was hampered by charge repulsion between the already deposited Al_2O_3 particles and other Al_2O_3 particles from suspension (Al_2O_3 colloids form a stable suspension, as is shown by the relatively high zeta-potential of the particles at neutral pH).

One other reason for the limited flux decline could be the limited hydraulic resistance of the Al_2O_3 foulant cake. From particle size analysis of the aluminum oxide colloids, it is clear that the average size is approximately 139.4 nm, which is much larger than the membrane pore size (around 0.71 nm [44]). As such, it is likely that the fouling layer has large pores and a high porosity. As such, it is possible that the aluminum oxide fouling layer would not result in a significant hydraulic resistance compared to the membrane resistance.

No significant effects on flux were measured when CaCl_2 was present in the feed solution, possibly because there is no specific interaction between calcium ions and colloids. This could be expected, since positively charged colloids are not expected to show significant interactions with multivalent cations.

4.1.3. Fouling by latex

Fouling experiments with negatively charged latex colloids were also conducted under similar experimental conditions. Results are shown in Figure 4.3.

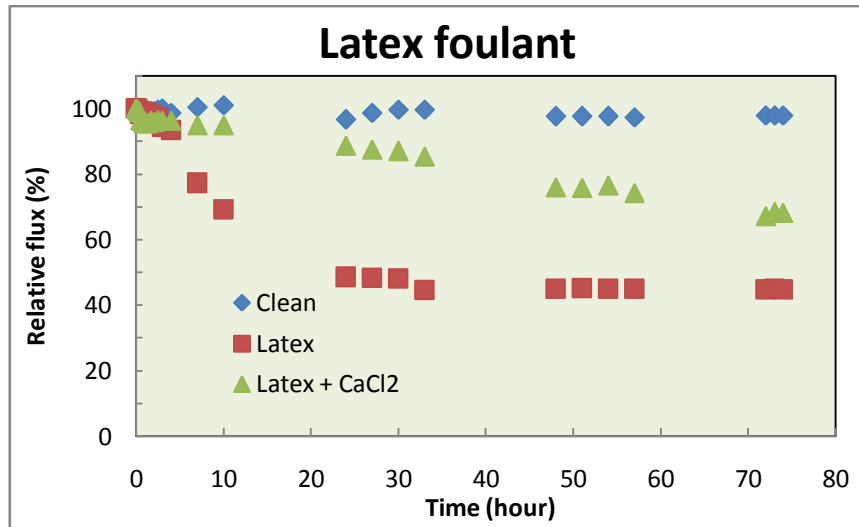


Figure 4.3: Relative flux as a function of time for latex fouling experiments with and without CaCl₂

It can immediately be seen in Fig 4.4 that the flux decline is much more clearly detectable compared to the experiment with Al₂O₃ particles, especially when CaCl₂ is absent in the solution.

As an evidence of this, the permeate flux rapidly dropped by around 52% after 24 hours of operation before the relative flux leveled off until the end of the experiment (most probably due to a depletion of latex in the bulk feed). In contrast, as shown above, permeate flux in the experiments with aluminum oxide was almost constant.

It is thus clear that latex settles onto the negatively charged membrane much more easier than positively charged Al₂O₃-particles. Although this is surprising, one possible explanation for this might be the lower charge of the latex particles compared to Al₂O₃. This will lead to less charge repulsion between the latex colloids amongst themselves, and most probably lead to a faster build-up of fouling beyond the monolayer coverage. In this case, monolayer coverage of the negatively charged particles on the negatively charged membranes might be the most difficult step, but further settling of particles might be faster than is the case for Al₂O₃.

Also the influence of CaCl_2 on the flux decline might indicate that charge repulsion and thus stability of the colloids plays an important role: when Ca^{2+} is added, the charge of the colloids becomes almost completely screened. This results in less fouling compared to the case where no CaCl_2 is present. This is surprising, but might be due to the size of the colloidal latex when CaCl_2 is present.

It is thus clear that there will be a coverage of latex colloids onto the membrane. These can however lead to flux decline in two different manners: firstly, there could be an increased hydraulic resistance due to the cake. However, it is unlikely that this cake resistance will be very high, since the latex particles are in the same size range as the Al_2O_3 -particles, and there no significant hydraulic resistance was observed.

Secondly, the flux could be declined due to the effect of cake-enhanced concentration polarization. When there is a cake layer of latex colloids on the membrane, the concentration of salts at the membrane surface will increase due to decreased back-diffusion, leading to a higher osmotic pressure difference and thus a lower flux. The fact that this CECP is more pronounced for latex is probably due to the larger deposits of colloids on the membrane surface compared to Al_2O_3 . It could also be due to a charge effect: once salts are rejected by the membrane (due to charge repulsion with the negative membrane), they have to diffuse back through the colloidal layer. Since latex, just as the membrane, is also negatively charged, this back-diffusion will also be hindered by charge repulsion, leading to more hindered back-diffusion and higher CECP. For Al_2O_3 -particles, the charge of the colloids is positive, and there will be less charge repulsion with negative charged ions rejected by the negatively charged membrane, leading to higher back-diffusion and thus less CECP.

4.1.4. Fouling by sodium alginate

Fouling experiments with sodium alginate (SA) were also carried out under the same experimental conditions, with both the presence and absence of CaCl_2 . Relative flux curves are shown in Figure 4.4.

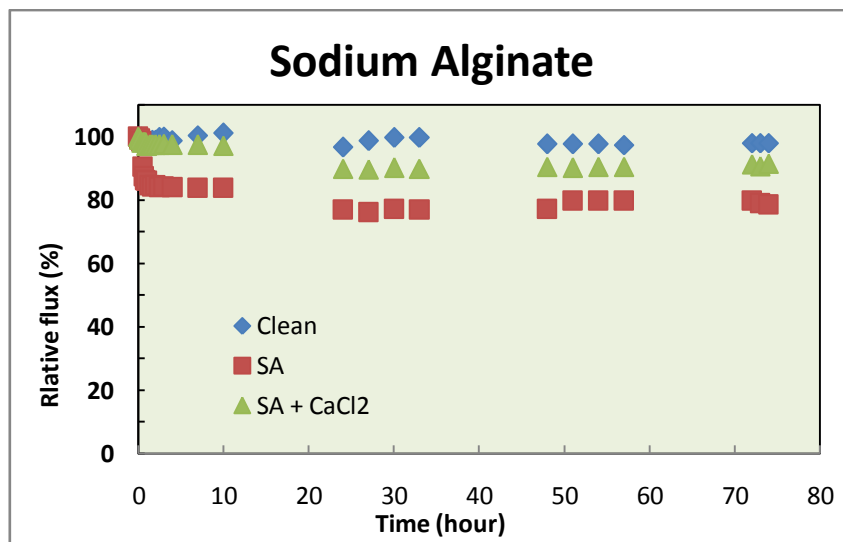


Figure 4.4: Relative flux as a function of time for SA fouling experiment with and without CaCl₂

SA alone induced a noticeable flux decline, although it was less pronounced than for latex. As shown, the flux for NF 270 membrane fouled by SA quickly dropped by about 12% within 4 hours after the start of filtration. Afterwards, the flux decline was more gradual and after one day of filtration, up to the end of the experimental run, the permeate flux remained constant. This can again be explained by two reasons, including CECP and an increased hydraulic resistance. Results seem to indicate that a combination of the two phenomena is the most plausible reason: the flux is immediately lowered at the beginning of the experiment and does not seem to decline further. This would indicate that there is an immediate fouling layer formed by sodium alginate, which leads to increased hydraulic resistance and increased CECP. However, the cake build-up is limited, since the flux does not decline further over time.

The presence of calcium ions has been shown in other studies to induce an extra permeate flux decline for filtration of SA [45,46]. However, in this study, the combination with CaCl₂ actually resulted in less flux decline. The most probable reason is that the presence of calcium ions in the concentrations used in this experiment caused a gel layer formation of SA. This has been described before in literature as the 'egg-box' model. In our case, the gel-like calcium-alginate complex appears to have a lower

hydraulic resistance to membrane flux compared to the experiment without CaCl_2 . Indeed, from a study conducted by van de Ven et al. on sodium alginate [4747], the lower hydraulic resistance in the presence of CaCl_2 can be explained by two reasons. Firstly, it was observed that the viscosity was lower for SA solutions with the addition of CaCl_2 compared to the case without CaCl_2 . This lower viscosity resulted in a lower value for resistance (Equation 2.4). The second reason is due to the size of the SA due to aggregation when adding CaCl_2 (see attachment). Larger particles cause a more open fouling layer than smaller ones, which leads to a lower hydraulic resistance.

4.1.5. Fouling by combined foulants

Foulants were mixed in the feed solution with the same concentrations used for experiments with single foulant. The relative flux data of mixtures of selected foulants as a function of time are plotted in Figure 4.5.

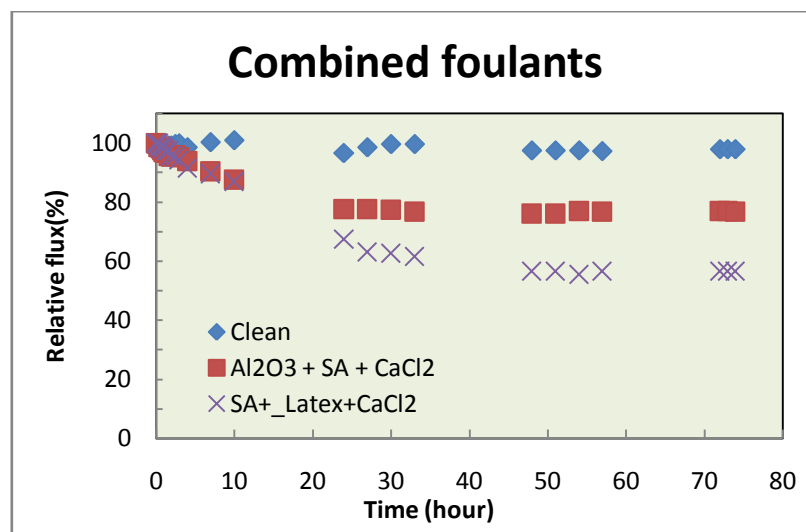


Figure 4.5: The evolutions of permeate fluxes in combined fouling experiments.

The difference in flux decline within the first hours was indistinguishable for the two fouling experiments. After 10 hours, the flux reduction in combined fouling experiment of SA + Latex + CaCl_2 started to be more detrimental than that of Al_2O_3 + SA + CaCl_2 , with

the values of relative flux at the end of the experiments ending at approximately 56% and 76% of the initial flux, respectively.

In detail, in comparison with fouling experiments of individual aluminum oxide and individual sodium alginate, the combination of foulants caused a greater flux reduction which indicates a synergistic effect on flux. As was shown for the flux decline with alginate, both CECP and increased hydraulic resistance had an influence of flux. For Al_2O_3 , no significant flux decline was observed. However, in the case of the combined fouling, Al_2O_3 seems to aggravate the flux decline, indicating that combination of Al_2O_3 with alginate leads to more severe CECP, or more severe hydraulic resistance. However, at this point, it is unclear what the main fouling mechanism is.

The same holds for the combination of latex and sodium alginate. The flux decline is lower than the separate flux declines observed for the separate foulants. Again, at this point, it is unclear what the main fouling mechanism is.

4.2. EFFECTS OF MEMBRANE FOULING ON INORGANIC SALT REJECTION

4.2.1. Salt rejection of clean membrane

The effects of membrane fouling on the membrane behavior and separation efficiency were further examined by comparing the salt rejection values of the clean and the fouled membranes. The salt rejection was calculated based on Equation 3.1 and the measured conductivity values of the feed and the permeate which were measured throughout the experimental runs. The evolution of salt rejection by the clean membrane is represented in Figure 4.6.

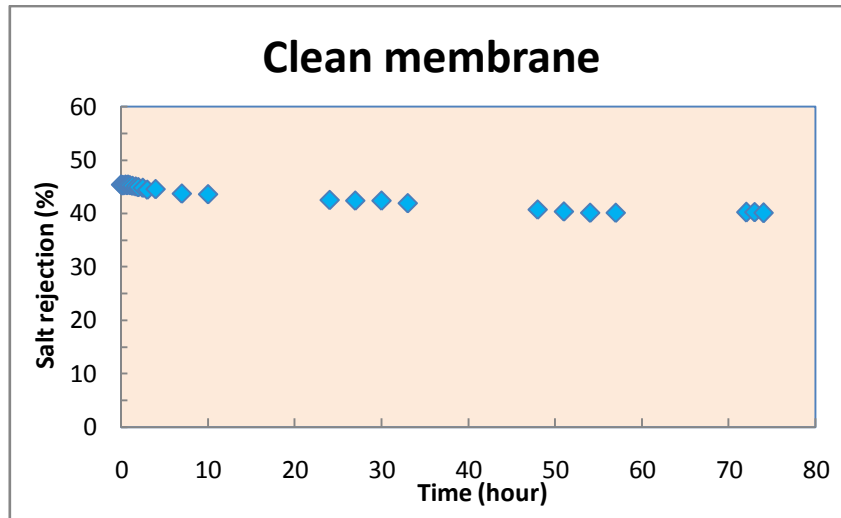


Figure 4.6: Salt rejection for clean membrane as a function of time

Figure 4.6 shows the rejection value of salt for the unfouled membrane. The observed NaCl rejection of the NF 270 membrane at the start of the experiment was 45.4%, which is relatively consistent with the data given by the manufacture, which shows in Table 3.3.

It's clearly seen that the salt rejection was reduced over filtration time even in case of virgin membrane. This phenomenon may be explained by the change of feed volume at the end of the experiment compared to the initial volume. In fact, there were 26 permeate samples which the volume of 20ml for each were taken for the latter TOC analysis in each experiment and therefore, the volume of the feed was gradually lost during the filtration. This leads to the increase in the feed concentrations over time and a lower salt rejection was observed. The result was in accordance with a finding in a study of S. Lee et al. [48].

4.2.2. Salt rejection of fouled membranes

Salt rejection of the fouled membranes is further discussed in term of reduction of salt rejection over time. The reduction of rejection is equal to the difference of salt rejection values at the start and the end of each experimental run. These values are plotted for all membranes (also for the clean membrane) in Figure 4.7.

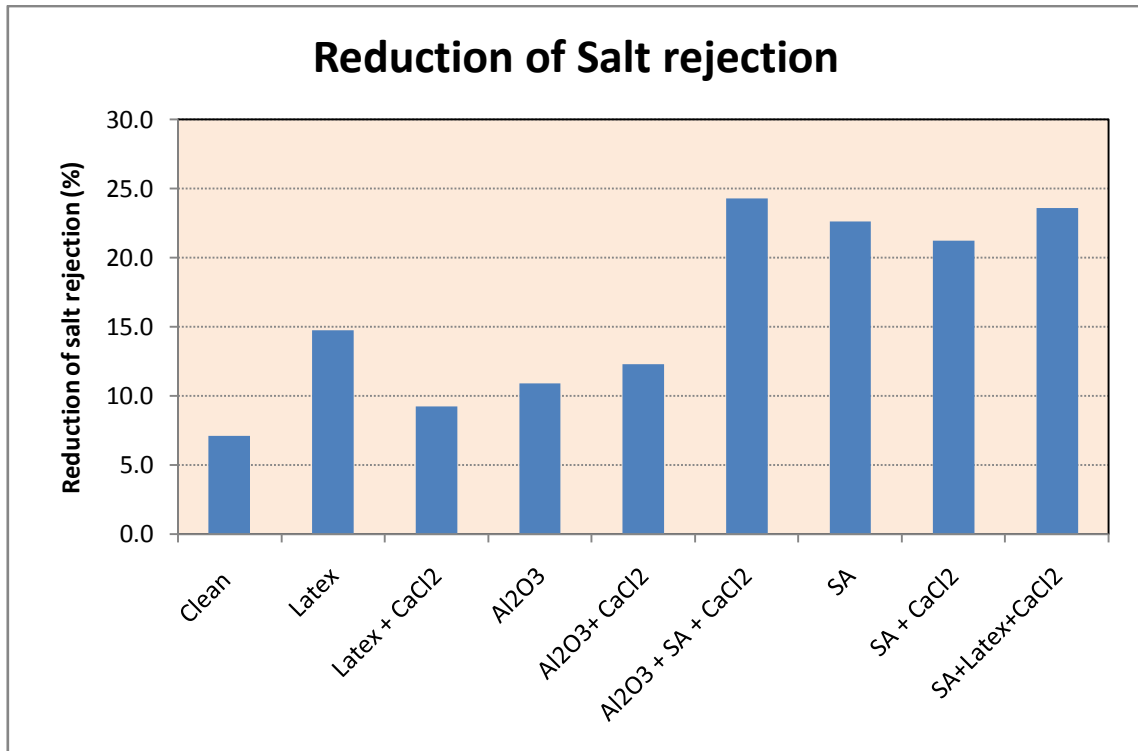


Figure 4.7: The reduction of salt rejection of clean membrane and different fouled membrane

The obtained results appear to shed more light on what the dominant fouling mechanisms are for the different foulants. Since cake-enhanced concentration, when present, will lead to increased concentrations of salts at the membrane surface, this CECP will also lead to lower observed rejections.

As is clear from Figure 4.8, there is only a slightly higher decrease in rejection for Al₂O₃-fouled and latex fouled membranes compared to the clean membrane. This would seem to indicate that for these foulants, no CECP is present. Thus, the main reason for the flux declines are most probably due to increased hydraulic resistances. Since the sizes of latex and Al₂O₃ are more or less the same, the specific cake resistance (hydraulic resistance per unit cake thickness) of the two colloids should be the same. Therefore, since latex membranes show more flux decline, it is evident that the latex cakes are thicker than the cakes formed by Al₂O₃. As stated above, this is probably due to the stability of the colloids. Since Al₂O₃-particles have a higher surface charge, there will be

more resistance against high cake-layer height build-up, due to Al_2O_3 - Al_2O_3 repulsion. For latex, the surface charge is lower, and even lower in the case when CaCl_2 is also added, thus leading to more deposits on the membrane surface and a thicker cake. When CaCl_2 is present, however, the colloids will cluster, and result in a cake with a larger porosity. This leads to less hydraulic resistance than for the case where no CaCl_2 is present, however, cake formation and increased hydraulic resistance are still the main reasons for flux decline (not CECP).

As can be clearly seen from Figure 4.8, as a single foulant in the feed, SA fouling does significantly reduce the salt rejection efficiency. Apparently, the fouling layer formed by the deposition of SA on the membrane surface, does increase the salt concentration at the membrane surface dramatically. This means that the back-diffusion of salts through the alginate cake must be much smaller than the back-diffusion in the case of latex and aluminum oxide. This is highly plausible, since alginate forms a more gel-like layer on the membrane, with less porosity and higher tortuosity compared to the colloidal cakes. As such, fouling by alginate is most likely due to a combination of cake-enhanced concentration polarization and increased hydraulic resistance. The fact that hydraulic resistance also plays an important role, is demonstrated by the fact that the salt rejection declines in a similar manner for the SA-fouled membrane as for the SA-fouled membrane in the presence of CaCl_2 , indicating that CECP is the same for both fouled membranes. However, due to the larger particle size of alginate in the presence of CaCl_2 , the hydraulic resistance of the cake is lower in the presence of CaCl_2 , leading to lower flux declines.

It is interesting to note that the mixtures of sodium alginate with aluminum oxide or latex also caused similar behaviors on rejection as just alginate. In contrast, the flux results showed a worse behavior when alginate was combined with both of the foulants. This also confirms the hypotheses about fouling mechanisms mentioned above. Since Al_2O_3 has no hydraulic resistance and does not cause CECP, both the effects on flux and on rejection in the combined fouling of Al_2O_3 and alginate are caused by alginate, which has CECP and increased hydraulic resistances. Since no increased CECP is seen in the combined fouling runs compared to the alginate fouled membranes (since no significant

difference in salt rejection compared to the alginate fouled membrane is seen), Al_2O_3 mainly appears to have an effect on the hydraulic resistance. A combination of Al_2O_3 colloids with alginate in between, apparently causes a higher hydraulic resistance without affecting CECP.

For latex, a similar observation can be made. This is quite logical, since the effect of latex on flux appeared to be mainly an increased hydraulic resistance effect, without effect on CECP.

4.3. REJECTION OF CARBAMAZEPINE

4.3.1 Rejection of carbamazepine by clean membrane

The rejection of carbamazepine in Milli-Q water was studied to obtain the base line rejection values of the virgin membrane during 74 hour filtration. Since carbamazepine is an uncharged organic solute, its transport through the NF membrane is only due to size exclusion interactions, and non-electrostatic solute-membrane affinity. Size exclusion interactions are usually quantitatively expressed by comparing the size of the solute (molecular weight) to the so-called molecular weight cut-off (MWCO) of the membrane. This MWCO is a value given by the manufacturer, and is a value for the molecular weight expressed in g/mol, indicating the molecular weight of the smallest hypothetical non-charged solute that has a rejection of at least 90% [49]. Based on the data given by the manufacturer (see Table 3.3) the NF 270 membrane investigated has a MWCO value of 200 – 300 Dalton, whereas the molecular mass of carbamazepine is 236.28 g/mol. Hence, carbamazepine could not be completely rejected by this membrane due to size exclusion effects. This is also illustrated in Figure 4.8: the initial rejection is 74.2 % and this value slightly dropped to approximately 70% at the end of the experimental run (due to the increase in concentration due to sampling). In a recent study, similar rejection values for carbamazepine were found by Hajibabania et al. (73%) [48].

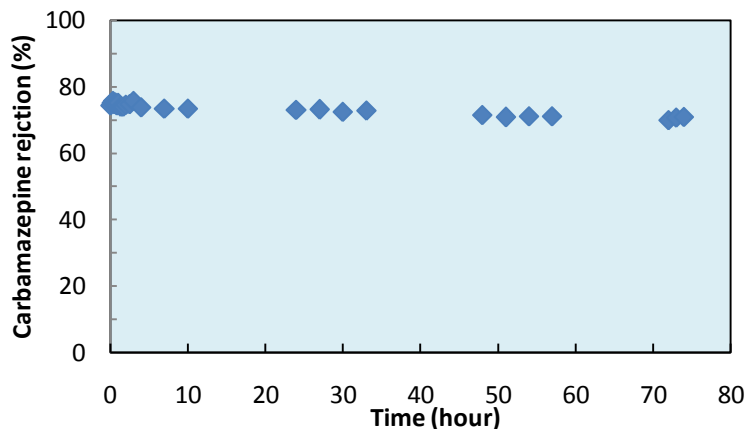
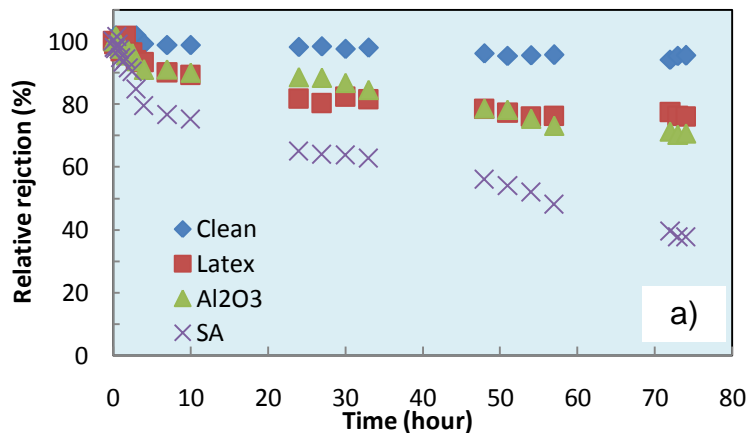


Figure 4.8: Experimental values for carbamazepine rejection by the clean membrane as a function of time

Besides size exclusion effects, also non-electrostatic solute-membrane affinity will have an effect on rejection. This will be dealt with in a further paragraph.

4.3.2 Rejection of carbamazepine by fouled membranes

Carbamazepine rejection of the fouled membranes is given in Figure 4.9. Fouling obviously reduced the removal efficiency of this non-ionic hydrophobic trace organic. However, the magnitude of decrease in rejection of carbamazepine was different for the different foulants because of their different characteristics such as different size, charge and hydrophobicity, and thus a different effect on membrane fouling as well.



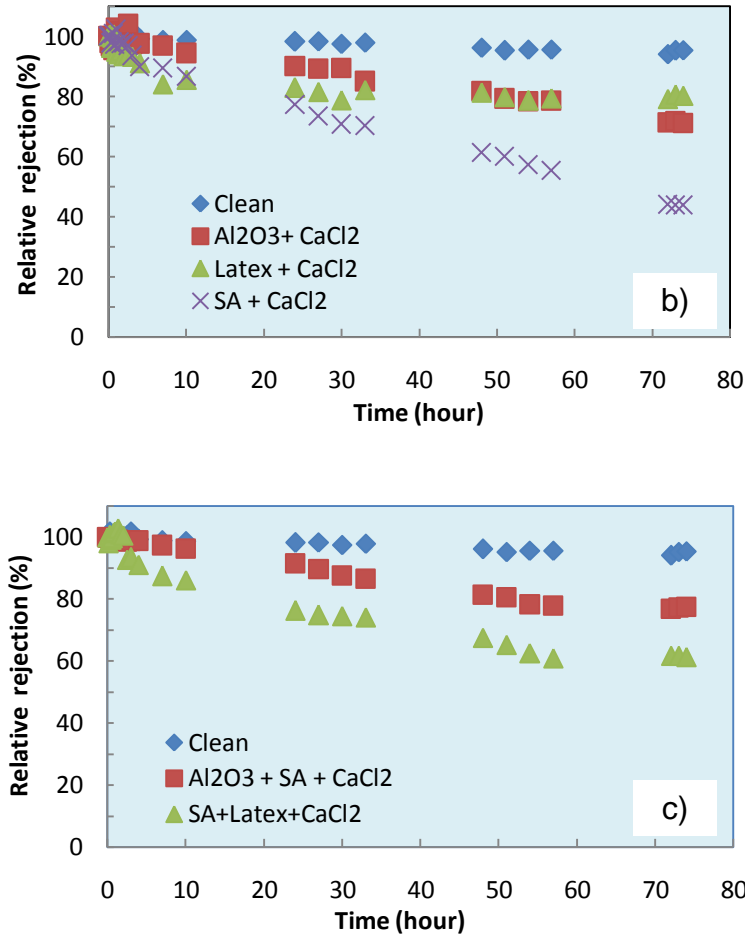


Figure 4.9: Carbamazepine rejection behavior of fouled membrane with (a) the absence of CaCl₂, (b) the presence of CaCl₂ and (c) combined foulants.

Figure 4.9a clearly shows that fouling layers of latex and aluminum oxide induced an apparent decrease in the rejection of carbamazepine, which the values of relative rejection at the end of the experimental runs were 75.9% and 70.6% respectively. However, the curves describing the changes of carbamazepine rejection by these two foulants are relatively similar. This is consistent with the effects of fouling on salt rejection for these foulants.

The change in retention of carbamazepine in the presence of SA fouling was much more pronounced than individual aluminum oxide or latex fouling. For instance, the rejection of carbamazepine by SA fouled membrane decreased to 37.6% after 74 hour of filtration. The decrease in rejection by SA fouling is consistent with the results obtained

by Hajibabania et al [48], and also agrees with the larger changes in salt rejection for the alginate fouled membranes compared to the colloidal fouled membranes.

To get more insight in the effects of fouling on rejection of carbamazepine, changes in salt rejection with fouling were compared to changes in carbamazepine rejection with fouling in Figure 4.10.

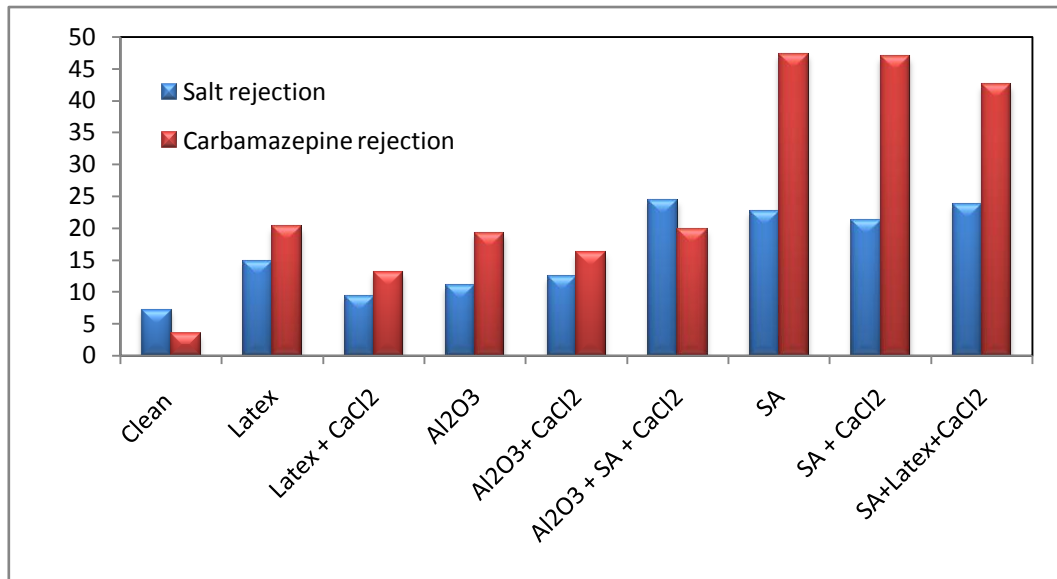


Figure 4.10: Comparison between the reduction of salt rejection and carbamazepine rejection

It is clear from this figure that for most foulants, the reduction of salt rejection and carbamazepine rejection follow more or less similar trends. This indicates that similar fouling mechanisms that affect rejection are at hand. Therefore, similar explanations can be used for the decrease in carbamazepine rejection, as were used to explain the changes in salt rejection above.

However, there are some slight inconsistencies between the changes in salt rejection and changes in carbamazepine rejection. Firstly, the decreases in carbamazepine rejection for the SA-fouled membranes are much higher than the decrease in salt rejection. This is also the case for the membrane fouled with SA+Latex+CaCl₂. For the

membrane fouled with SA+Al₂O₃+CaCl₂, on the other hand, this difference between the decrease in salt rejection and carbamazepine rejection was not observed.

This would seem to indicate that, although similar fouling mechanisms and influences on rejection are at hand, there is another mechanisms playing a role for carbamazepine rejection compared to salt rejection. This mechanism may be the non-electrostatic interaction between the carbamazepine and the fouling layer, which can be calculated from the surface tension values. Therefore, in the following paragraph, rejection values are plotted as a function of interaction energies.

4.7. CARBAMAZEPINE-MEMBRANE AFFINITY

Table 4.4 gives an overview of the free energies of interaction, ΔG_i , between carbamazepine and the clean and fouled membranes, calculated from contact angle values to evaluate the affinity between them.

Table 4.4: Surface tension components and the free-energy of intertactions for clean and fouled membranes

Name	γ^{LWM}	γ^{+M}	γ^{-M}	γ^{tot}	ΔG_i ($\times 10^{-18} J$)
Clean membrane	38.62	1×10^{-6}	42.01	38.63	2.53
Al ₂ O ₃	41.97	1×10^{-6}	17.90	41.98	-2.39
Al ₂ O ₃ + CaCl ₂	41.13	3.29	9.61	52.39	-5.07
Latex	40.93	1×10^{-6}	3.74	40.94	-7.06
Latex + CaCl ₂	37.49	1×10^{-6}	1×10^{-6}	37.47	-10.9
SA	31.02	1×10^{-6}	17.24	31.03	-1.63
SA + CaCl ₂	37.47	2.49	1×10^{-6}	37.48	-1.11
SA + Latex + CaCl ₂	39.89	1×10^{-6}	18.87	37.90	-1.99
SA + Al ₂ O ₃ + CaCl ₂	47.54	4.21	1×10^{-6}	47.54	-12.0

For the clean membrane, the free energy of interactions positive, indicating that no spontaneous partitioning of carbamazepine into the membrane due to solute-membrane affinity will occur. Consequently, the rejection of carbamazepine by the virgin membrane was relatively high, since non-electrostatic repulsion was present in addition to steric effects.

In contrast to the clean membrane, all fouled membranes (or at least the fouling layers on top of the membranes), have significant affinity for carbamazepine, as can be seen from negative values of ΔG_i in Table 4.4. This confirms that the transfer of carbamazepine to the membrane will be facilitated in the presence of fouling layer which could give an indication for the lower rejection values of carbamazepine observed for the fouled membranes.

In the results shown above, it was shown that carbamazepine rejection closely followed salt rejection for the colloidal fouled membranes, but a higher decrease in rejection was seen for carbamazepine compared to the salt rejection for all sodium alginate fouled membranes (including the combined foulants), except for the combined fouling with Al_2O_3 and sodium alginate. Since the colloidal fouled membranes show similar trends for carbamazepine and salt rejection, the same mechanisms of rejection and influence of fouling on rejection apply.

For the SA fouled (including combined fouling) membranes, however, an extra mechanism seems to play a role. This could be the effect of non-electrostatic solute membrane affinity. When carbamazepine rejection differences with the clean membrane are plotted for all the sodium-alginate fouled membranes as a function of solute-membrane interaction, it is clear that the SA-fouled, the SA+CaCl₂ fouled and the SA+Latex+CaCl₂ fouled membranes all have similar behavior and more or less similar interaction energies. For the SA+Al₂O₃+CaCl₂ fouled membrane, however, there is a much more intense interaction (attraction) between the carbamazepine and the foulant.

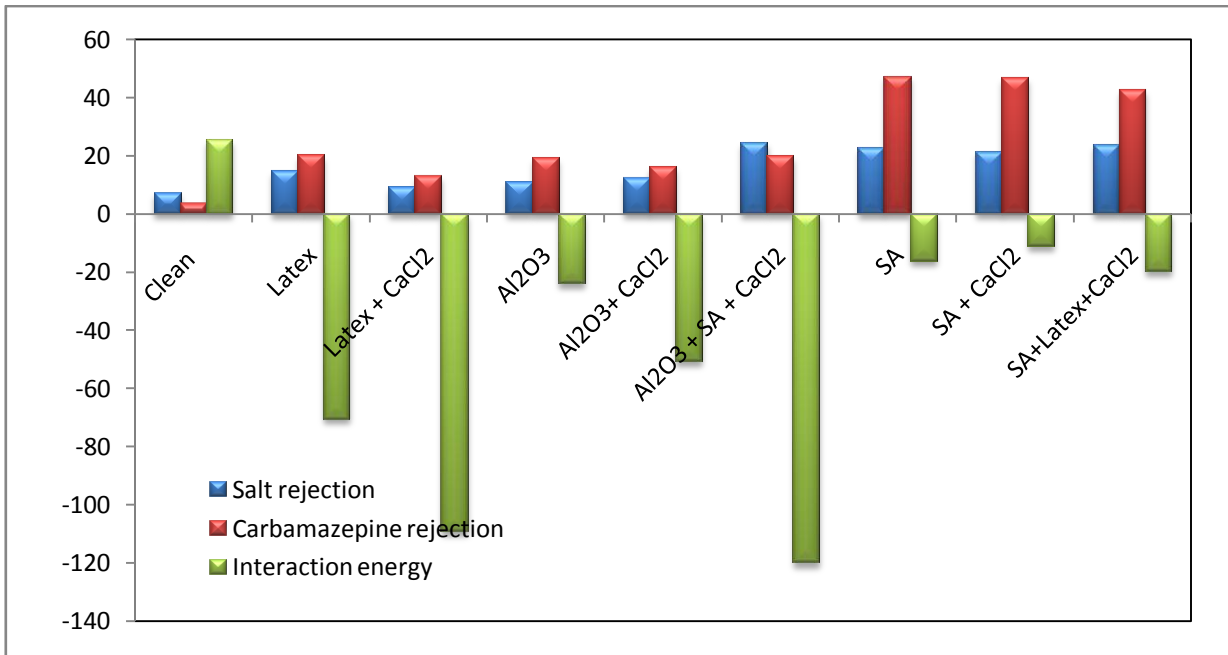


Figure 4.11: The reductions of salt rejection and carbamazepine rejection vs. interaction energy

This could be a hint at what is happening for the fouled membranes. For the colloidal fouled membranes, there is no clear effect that CECP is playing a role. For all SA-fouled membranes, however, it has been shown that CECP is indeed affecting rejection. It could be theoretically expected that if carbamazepine shows more affinity for the foulant, this would lead to more pronounced CECP. However, here, an opposite trend seems to emerge. This can be explained as follows: convective drag of carbamazepine towards the membrane will not be significantly altered by the interaction energy between carbamazepine and the foulants, since the driving force for permeation through the large pore size of the fouling layer is relatively high. However, the interaction energy will have a pronounced effect on back-diffusion, since the driving force for back-diffusion is much lower. Therefore, it is expected that for the fouling layers which have a higher affinity for carbamazepine, the back-diffusion will occur much faster than for the other foulants, since the solute is attracted by the foulant and thus partitions back to the feed through the foulant layer much easier. This explains the completely different trends seen for SA+Al₂O₃+CaCl₂ compared to the similar behavior of all the other SA-fouled membranes.

CONCLUSIONS AND RECOMMENDATIONS

5.1. CONCLUSIONS

In this dissertation, three types of foulants were used to simulate membrane fouling and to assess the impact of fouling on the rejection of carbamazepine by NF/RO membranes.

- The reported result indicated that the largest flux decline was observed when the membrane was fouled by latex colloids. However, there was no flux decline observed on filtration of feed water containing aluminum oxide particles. The flux decline behavior with sodium alginate was in between that of these two foulants. The presence of calcium chloride generally improved the fluxes in both experiments with sodium alginate and latex, compared to that of the individual foulant. With combined fouling experiments, the fluxes illustrated synergistic effects of combined foulants but the flux declines are not as significant as latex.
- Aluminum oxide and latex were only caused a slight decrease since there was no presence of cake-enhanced concentration polarization. Nevertheless, sodium alginate caused the most remarkable loss in salt rejection which can be explained by the strong impact of alginate cake to the hindrance of back – diffusion of salt. This was also hypothesized that the same fouling mechanisms induced the similar behaviors for the combinations of sodium alginate with aluminum oxide and latex.
- Interestingly, the carbamazepine rejection almost followed the trends of salt rejection. This indicated that the existence of similar fouling mechanisms between carbamazepine and salt rejection.
- In term of free energies of interactions (ΔG_i), all fouled membranes had negative values which showed a significant affinity to carbamazepine and therefore, lower

rejection values were observed. It was concluded that non-electrostatic solute-membrane affinity played a crucial role for the sodium alginate fouled membranes. It was concluded that non-electrostatic solute-membrane affinity played a crucial role for the sodium alginate fouled membranes. Indeed, the interaction energy have significantly effects on the back-diffusion since the driving force for the back-diffusion is much lower compared to that of the permeate flow. Back-diffusion is likely to occur much faster for fouling layers have a high affinity for carbamazepine.

5.2. RECOMMENDATIONS FOR FUTURE WORKS

Based on the conclusions obtained in this study, the following recommendations are made for future works:

- This study was carried out with only carbamazepine in the feed water. In practice, there are other trace organic contaminants detected in high concentrations in drinking water resources. Some of the contaminants which may pose a health risk to human beings, include sulfamethoxazole, bisphenol A, N-nitrosodimethylamine, 17 β -Estradiol and so on. More experiments with a wide range of solutes with varying physico-chemical properties will give a clearer observation about the influence of fouling on their removal.
- Future research should include atomic force microscopy (AFM) and scanning electron microscopy (SEM) analysis of fouled membranes in order to elucidate the thickness of the cake layers, as well as the levels of coverage of the membranes by the foulants.
- A model that predicts rejection of organics by high pressure membrane in water purification has been introduced before been introduced, by Verliefde et al.(2009).However, it becomes clear from the experiments carried out here that this model is only applicable for clean membranes and not always efficient in predicting observed behavior when the membranes are fouled. Therefore, there is a need for development of models that will predict and explain behavior of NF/RO

membrane when they are fouled by colloids, natural organic matter and combinations of such foulants. Based on result of this study, a mathematically model for prediction of organic pollutants removal by these types of foulants should be considered and published in the future. One possible way of doing this, would be to deal with the foulant layer as a secondary membrane on the dense membrane, and integrate the convection-diffusion equation not only over the membrane, but on the combined system of membrane and fouling layer (a “membrane-in-series” model).

REFERENCES

1. T. Heberer. Occurrence, fate and removal of pharmaceutical residues in the aquatic environment: a review of recent research data. *Toxicology letters* **131** (2002), 5 – 17.
2. P.Xu, J.E. Drewes, T.U. Kim, C. Bellona, G. Amy. Effect of membrane fouling on transport of organic contaminants in NF/RO membrane applications. *Journal of Membrane Science* **279** (2006), 165-175.
3. A.E. Contreras, A. Kim and Q. Li. Combined fouling of nanofiltration membranes: mechanisms and effect of organic matter. *Journal of Membrane Science* **327** (2009), 87 – 95.
4. A.R.D. Verliefde, E.R. Cornelissen, S.G.J.Heijman, I.Petronic, T.Luxbacher, G.L.Amy, B.V.D. Bruggen, J.C.V. Dijk. Influence of membrane fouling by (pretreated) surface water on rejection of pharmaceutically active compounds (PhACs) by nanofiltration membranes. *Journal of Membrane Science* **330** (2009), 90 - 103.
5. R.D. Cohen and R.F. Probstein. Colloidal fouling of Reverse Osmosis Membranes. *Journal of Colloid and Interface Science*, **114** (1986), 194 – 207.
6. E.M.V. Hoek, A.S. Kim, M. Elimelech. Influence of crossflow membrane filter geometry and shear rate on colloidal fouling in reverse osmosis and nanofiltration separations. *Environmental Engineering Science* **19** (2002), 357 – 372.
7. H.Y. Ng, M. Elimelech. Influence of colloidal fouling on rejection of trace organic contaminants by reverse osmosis. *Journal of Membrane Science* **244** (2004), 215 – 226.
8. S.G. Yiantsios and A.J. Karabelas. The effect of colloid stability on membrane fouling. *Desalination* **118** (1998), 143 – 152.
9. X.Zhu and M.Elimelech. Fouling of reverse osmosis membranes by aluminum oxide colloids. *Journal of environmental engineering* (1995), 884 – 892.
10. L.D. Nghiem, S. Hawkes. Effect of membrane fouling on the nanofiltration of pharmaceutically active compounds (PhACs): Mechanism and the role of membrane pore size. *Separation and Purification Technology* **57** (2007), 182 – 190.
11. S.G. Yiantsios, D. Sioutopoulos, A.J. Karabelas. Colloidal fouling of RO membranes: an overview of key issues and efforts to develop improved prediction techniques. *Desalination* **183** (2005), 257 – 272.
12. L.D. Nghiem, P.J. Coleman, C. Espendiller. Mechanisms underlying the effects of membrane fouling on the nanofiltration of trace organic contaminants. *Desalination* **250** (2010), 682 – 687.

13. L.D. Nghiem, C. Espendiller, G. Braun. Influence of organic and colloidal fouling on the removal of sulphamethoxazole by nanofiltration membranes. *Water Science and Technology* **58** (2008), 163 – 169.
14. M. Mulder. Basic principles of membrane technology. Kluwer Academic Publishers (1996).
15. The world membrane separation technologies, Industry study with forecasts for 2012 and 2017. The Freedonia group (2009), 1 – 34.
16. W.R. Bowen, A.W. Mohammad and N. Hilal. Characterisation of nanofiltration membranes for predictive purposes use of salts, uncharged solutes and atomic force microscopy. *Journal of Membrane Science* **126** (1997), 91 – 105.
17. P.V.D Meeren. Membrane processes in environmental technology course note. Univeristy of Gent (2011).
18. B.V.D. Bruggen, L. Braeken, C. Vandecasteele. Flux decline in nanofiltration due to adsorption of organic compounds. *Seperation and Purification Technology* **29** (2003) 23 – 31.
19. S. J. Khan, J. E. Ongerth. Modelling of pharmaceutical residues in Australian sewage by quantities of use and fugacity calculation. *Chemosphere* **54** (2004), 355 -367.
20. M. S. Diaz-Cruz, M. J. L Alda, D. Barcelo. Environmental behavior and analysis of veterinary and human drugs in soils, sediments and sludge. *Trends in Analytical Chemistry* **22** (2003), 340 – 351.
21. Pharmaceuticals in our water supplies. <http://ag.arizona.edu/azwater/awr/july00/feature1.htm>. Last accessed on 5/15/2012.
22. N. Le-Minh, S.J. Khan, J.E.Drewes, R.M. Stuetz. Fate of antibiotics during municipal water recycling treatment. *Water Research* **44** (2010), 4295 – 4323.
23. J. Beausse. Selected drugs in solid matrices: a review of environmental determination, occurrence and properties of principal substances. *Trends in Analytical Chemistry, Vol 23* (2004), 10-11.
24. A.R.D. Verliefde, S.G.J Heijman, E.R.Cornelissen, G.L. Amy, B.V.D Bruggen and J.C.V Dijk. Rejection of trace organic pollutants with high pressure membrane (NF/RO). Volume **27** *Environmental Progress* (2008), 181 - 193.
25. B.V.D. Bruggen, C. Vandecasteele. Modelling of the retention of uncharged molecules with nanofiltration. *Water Research* **36** (2002), 1361-1365.
26. A.R.D. Verliefde, E.R.Cornelissen, S.G.J.Heijman, J.Q.J.C. Verberk, G.L. Amy, B.V.D Bruggen, J.C.V. Dijk. The role of electrostatic interaction on the rejection of organic solutes in aqueous solutions with nanofiltation. *Journal of Membrane* **322** (2008), 53.
27. C. Liu, S. Caothien, J. Hayes, T.Caothuy, T. Otoyoy, T. Ogawa. Membrane chemical cleaning: From art to science. *American Water Works Association MTC53852* (2001), 1-12.

28. C. Bellona, J.E. Drewes, P. Xu, G. Amy. Factors affecting the rejection of organic solutes during NF/RO treatment – a literature review. *Water Research* **38** (2004), 2795 – 2809.
29. K.S. Spiegler and O. Kedem. Thermodynamics of hyperfiltration (reverse osmosis): criteria for efficient membranes. *Desalination* **1**(1966), 311 – 326.
30. L. Puijker, M. Mons. Pharmaceuticals and personal care products in water cycle – international review. Kiwa report KWR 04. 013. Kiwa N.V. Water Research, Nieuwegein, The Netherlands, 2004.
31. C.D. Anderson and E.S. Daniels. *Emulsion Polymerization and Latex Applications*. (2003), 156p.
32. R. Duwadi. Electric field assisted ultrafiltration: modeling and experimental validation. Department of applied analytical and physical chemistry, Particle & Interfacial and Technology Group, Gent University (2009), 95p.
33. K. Kotcharaksa. The mechanisms, Products, and Kinetic of Carbamazepine-Free Chlorine Reactions. Faculty of the Virginia Polytechnic Institute and State University (2008), 1-45.
34. D. Fatta and A. Achilleos. Analytical methods for tracing pharmaceutical residue in water and wastewater. *Trends in Analytical Chemistry* **26** (2007), 515 – 533.
35. S. A. Snyder, J. Leising, P. Westerhoff, Y. Yoon, H. Mash and B. Vanderford. Biological and physical Attenuation of Endocrine Disruptors and Pharmaceuticals: Implications for Water Use. *Ground Water Monitoring and Remediation* **24** (2004), 108 – 118.
36. E.M.V. Hoek and M. Elimelech. Cake-enhanced concentration polarization: A new fouling mechanism for salt-rejection membranes. *Environmental Science & Technology* **37** (2003), 5581 – 5588.
37. K. Boussu, Y. Zhang, J. Coquyt, P.V.D. Meeren, A. Volodin, C.V. Haesendonck, J.A. Martens, B.V.D. Bruggen. Characterization of polymeric nanofiltration membranes for systematic analysis of membrane performance. *Journal of Membrane Science* **278** (2006), 418 – 427.
38. N. Hilal, H. Al-Zoubi, N.A. Darwish, A.W. Mohammad. Characterisation of nanofiltration membranes using atomic force microscopy. *Desalination* **177** (2005), 187 – 199.
39. K. Kontturi, M.Vouristo. Adsorption of globular proteins on polymeric microfiltration membranes. *Desalination* **104** (1996), 99 – 105.
40. A. Al-Amoudi, R.W. Lovitt. Fouling strategies and the cleaning system of NF membranes and factors affecting cleaning efficiency. *Journal of Membrane Science* **303** (2007), 4 - 28.
41. N.D. Lawrence, J.M. Perere, M. Iyer, M.W. Hickey and G.W. Stevens. The use of streaming potential measurements to study the fouling and cleaning of ultrafiltration membranes. *Separation and Purification Technology*, **48** (2006), 106 – 112.

42. A.R.D. Verliefde, E.R.Cornelissen, S.G.J.Hejiman, E.M.V. Hoek, G.L. Amy, B.V.D. Bruggen, and J.C.V. Dijk. Influence of Solute-Membrane Affinity on Rejection of Uncharged Organic Solutes by Nanofiltration Membranes. *Environmental Science and Technology* **43** (2009), 2400 – 2406.
43. J.A. Brant and A.E. Childress. Assessing short-range membrane –colloids interactions using surface energetic. *Journal of Membrane Science* **203** (2002), 257 – 273.
44. B.J. Marinas and R.E. Selleck. Reverse osmosis treatment of multicomponent electrolyte solutions. *Journal of Membrane Science* **72** (1992), 211 – 229.
45. R. Kummert and W. Stumm. The surface complexation of Organic acids on hydrous Al₂O₃. *Journal of Colloidal and Interface Science*, **75** (1986), 373 – 385.
46. S.J. Hwang, D.J. Chang, C.H.Chen. Steady-state permeate flux for particle cross-flow filtration. *The Chemical Engineering Journal* **61**(1996), 171 – 178.
47. W.J.C. Ven, K.V. Sant, I.G.M. Punt, A. Zwijnenburg, A.J.B. Kemperman, W.G.J. Meer, M. Wessling. Hollow fiber dead-end ultrafiltration: Influence of ionic environment on filtration of alginate. *Journal of Membrane Science* **308** (2008), 218 -229.
48. S. Hajibabania, A. Verliefde, J.E. Drewes, L.D. Nghiem, J. McDonal, S. Khan and P. Le-Clech. Effect of fouling on removal of trace organic compounds by nanofiltration. *Drinking Water Engineering and Science Discussions* **4** (2011), 117 – 149.
49. B.V.D. Bruggen, J. Schaep, D. Wilms, C. Vandecasteele. Influence of molecular size, polarity and charge on the retention of organic molecules by nanofiltration. *Journal of Membrane Science* **156** (1999), 29 – 41
50. S.Hong, R.S. Faibish and M. Elimelech. Kinetics of Permeate Flux Decline in Crossflow Membrane Filtration of Colloidal Suspensions. *Journal of Colloid and Interface Science* **196** (1997), 267 – 277.
51. L.D. Nghiem, A.I. Schafer and M. Elimelech. Role of electrostatic interactions in the retention of pharmaceutically active contaminants by a loose nanofiltration membrane. *Journal of Membrane Science* **286** (2006), 52-59.
52. A.R.D. Verliefde, S.G.J. Heiman, E.R. Cornelissen, G. Amy, B.V.D Bruggen and J.C.V. Dijk. Influence of electrostatic interactions on the rejection with NF and assessment of the removal efficiency during NF/GAC treatment of pharmaceutically active compounds in surface water. *Water research* **41** (2007), 3227 – 3240.
53. W. Norde, *Colloids and Interfaces in Life Sciences*. Dekker, New York, 2003.
54. G. Singh and L.Song. Quantifying the effect of ionic strength on colloidal fouling potential in membrane filtration. *Journal of Colloid and Interface Science* **284** (2005), 630 – 638.

55. M. Zhang and L. Song. Mechanisms and parameters affecting flux decline in cross-flow microfiltration and ultrafiltration of colloids. *Environmental Science and Technology*, **34** (2000), 3767 – 3773.
56. P.V.D. Meeren, H. Saveyn, S.B. Kassa, W. Doyen and R. Leysen. Colloid-membrane interaction effects on flux decline during cross-flow ultrafiltration of colloidal silica on semi-ceramic membrane. *Physical Chemistry Chemical Physics*, **6** (2004), 1408 – 1412.
57. M.A. Zazouli, M. Ulbricht, S. Nasser, H. Susanto. Effect of hydrophilic and hydrophobic organic matter on amoxicillin and cephalixin residuals rejection from water by nanofiltration. *Iranian Journal of Environmental Health Science and Engineering* **7** (2010), 15 – 24.
58. Q. Li, M. Elimelech. Synergistic effects in combined fouling of a loose nanofiltration membrane by colloidal materials and natural organic matter. *Journal of Membrane Science* **278** (2006), 72 – 82.
59. G. Artug, J. Hapke. Characterization of nanofiltration membranes by their morphology, charge and filtration performance parameters. *Desalination* **200** (2006), 178 – 180.
60. E.M. Vrijenhoek, S. Hong, M. Elimelech. Influence of membrane surface properties on initial rate of colloidal fouling of reverse osmosis and nanofiltration membranes. *Journal of Membrane Science* **188** (2001), 115 - 128.
61. J. Zhao and W. Brown. Surface Characteristics of Polystyrene Latex Particles and Comparison with Styrene-Butadiene Copolymer Latex Particles Using Dynamic Light Scattering and Electrophoretic Light Scattering Measurements. *Journal of Colloid and Interface Science* **179** (1996), 255 – 260.
62. W.S. Ang, A. Tiraferri, K.L. Chen, M. Elimelech. Fouling and cleaning of RO membranes fouled by mixtures of organic foulants simulating wastewater effluent. *Journal of Membrane Science* **376** (2011), 196 – 206.
63. A.V. Delgado, F. Gonzalez-Caballero, R.J. Hunter, L.K. Koopal, and J. Lyklema. Measurement and Interpretation of Electrokinetic phenomena. *Pure and Applied Chemistry* **77**, 1753 – 1805.
64. S.H. Belhrens and M. Borkovec. Influence of secondary interaction energy minimum on the early stages of colloidal aggregation. *Journal of Colloid and Interface Science* **225** (2000), 460 – 465.
65. K. Listiarini, W. Chun, D.D. Sun, J.O. Leckie. Fouling mechanism and resistance analyses of the systems containing sodium alginate, calcium, alum and their combination in dead-end fouling of nanofiltration membranes. *Journal of Membrane Science* **344** (2009), 244 -251.
66. J.W.S. Goossens and A. Zembrod. Characterization of the surface of polymer lattice by photon correlation spectroscopy. *Journal of Dispersion Science and Technology* **2** (1981), 255 – 266.

67. M.A. Zazouli, M. Ulbricht, S. Nasser, H. Susanto. Effect of hydrophilic and hydrophobic organic matter on amoxicillin and cephalexin residuals rejection from water by nanofiltration. *Iran. J. Environ. Health. Sci. Eng* **7** (2010), 15 – 24.
68. S. Lee, J. Cho, M. Elimelech. Influence of colloidal fouling and feed water recovery on salt rejection of RO and NF membrane. *Desalination* **160** (2004), 1 – 12.
69. L. Braeken, R. Ramaekers, Y. Zhang, G. Maes, B.V.D Bruggen, C. Vandecasteele. Influence of hydrophobicity on retention in nanofiltration of aqueous solutions containing organic compounds. *Journal of Membrane Science* **252** (2005), 195 – 203.
70. Y. Yoon, P. Westerhoff, S.A. Snyder, E.C. Wert. Nanofiltration and Ultrafiltration of endocrine disrupting compounds, pharmaceuticals and personal care products. *Journal of membrane Science* **270** (2006), 88.
71. A.J. Kerchove and M. Elimelech. Formation of Polysaccharides Gel layers in the Presence of Ca^{2+} and K^{+} ions: measurement and mechanisms. *Biomacromolecules* **8** (2007), 113 – 121.

APPENDIX

Table 1: Measured properties of the NF 270 membrane

Properties	Value
Permeability, l/m ² .h.bar	10.5
m/s	8.8x10 ⁻⁶
Contact angle	
water	42° ± 0.5°
glycerol	66° ± 1.3°
diiodomethane	33° ± 1.6°

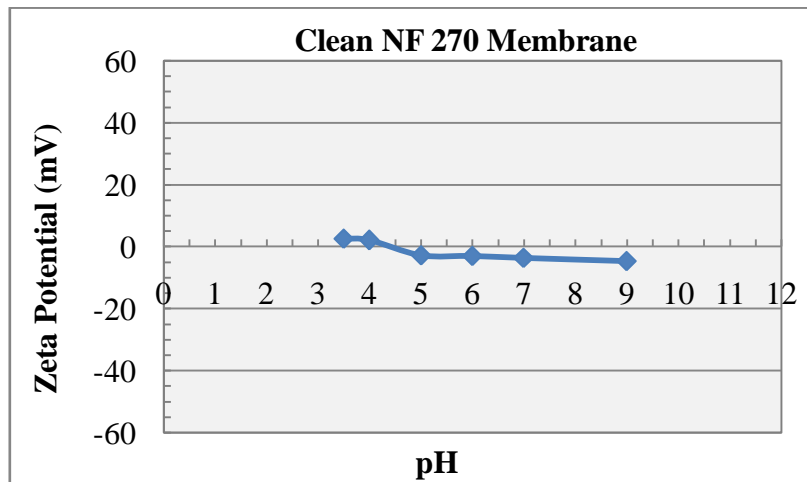


Figure 1: Variation of the zeta potential of NF 270 membrane with pH.

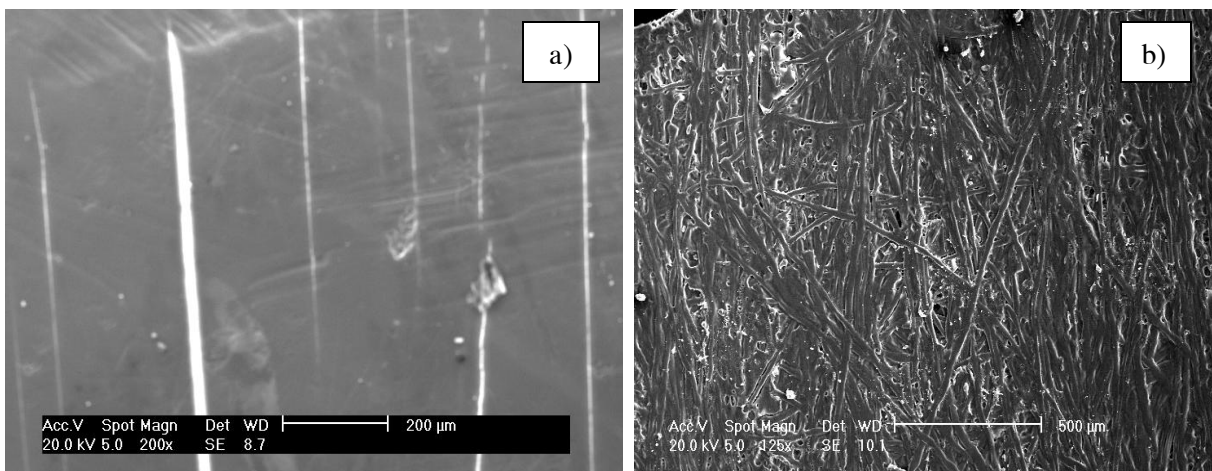


Figure 2: SEM images of the surface (a) and bottom (b) of NF 270 membrane

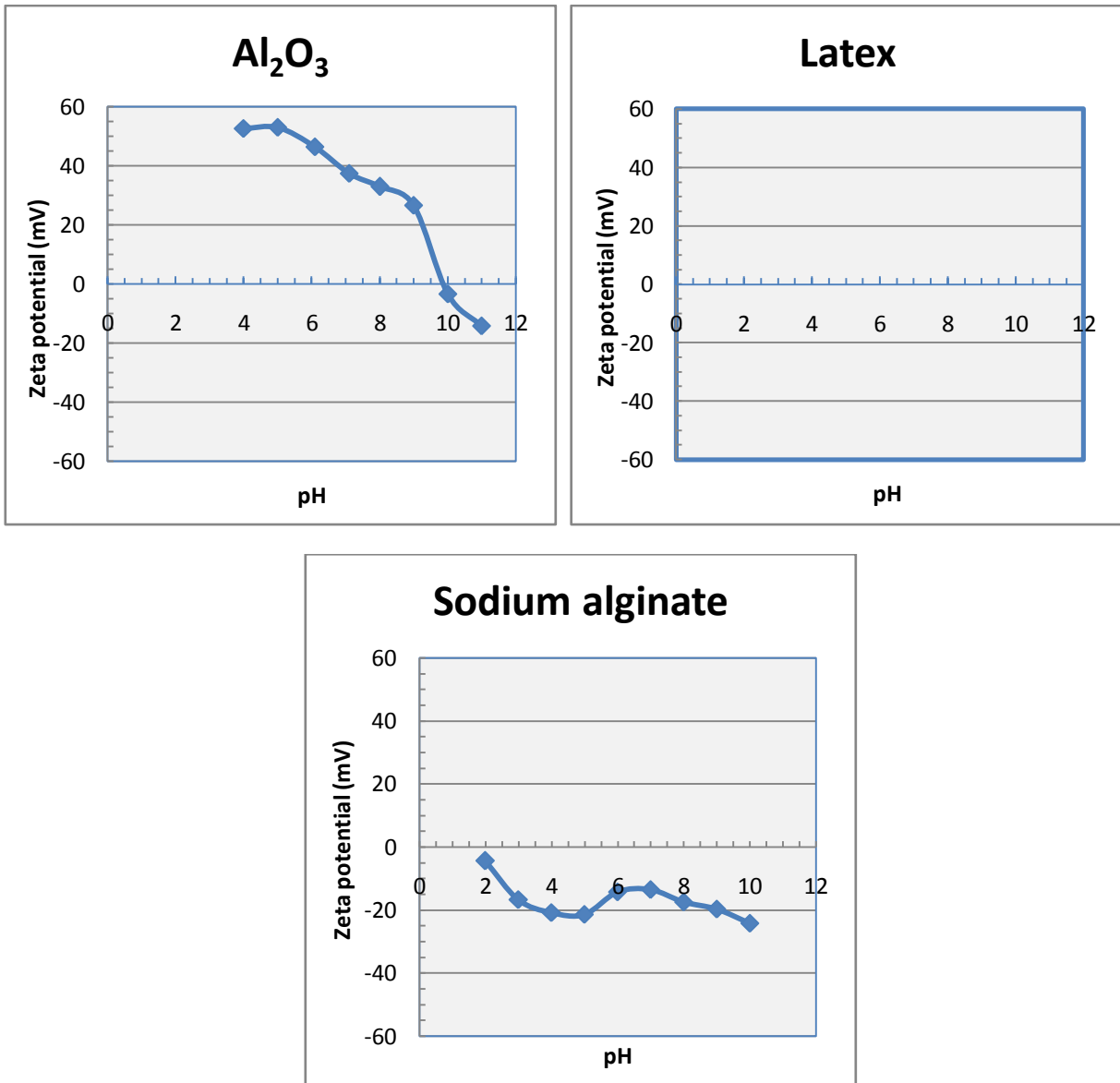


Figure 3: Zeta potential as a function of pH for Al₂O₃, sodium alginate and latex

Table 2: Particles size of different foulants

Foulants	Diameter (nm)	SD (nm)
Al ₂ O ₃	139.4	2.8
Al ₂ O ₃ + CaCl ₂	143.2	1.6
Latex	153.6	2.9
Latex + CaCl ₂	159.8	1.5
SA	300.7	5.4
SA +CaCl ₂	1938.0	1044.8
Al ₂ O ₃ +SA +CaCl ₂	198.0	2.1
Latex +SA+ CaCl ₂	178.8	1.0

Table 4: Contact angles of fouled membranes with three liquid probes

Fouling experiment	Diiodomethane (°)	Glycerol (°)	Water (°)
Al ₂ O ₃	28.2± 3.7	64.0±1.6	62.6±1.0
Al ₂ O ₃ + CaCl ₂	39.1±3.1	53.7±2.2	59.7± 2.8
Latex	31.9± 3.6	62.0±2.4	84.2±2.9
Latex + CaCl ₂	38.3± 3.2	91.1±2.5	77.7±2.9
SA	50.1±2.2	80.9±1.3	71.1±2.6
SA +CaCl ₂	43.4± 3.7	62.4±2.4	71.3±2.8
Al ₂ O ₃ +SA +CaCl ₂	18.3± 2.1	43.3±1.4	67.7±1.7
Latex +SA+ CaCl ₂	41.3±1.9	65.6± 1.8	61.8±1.3